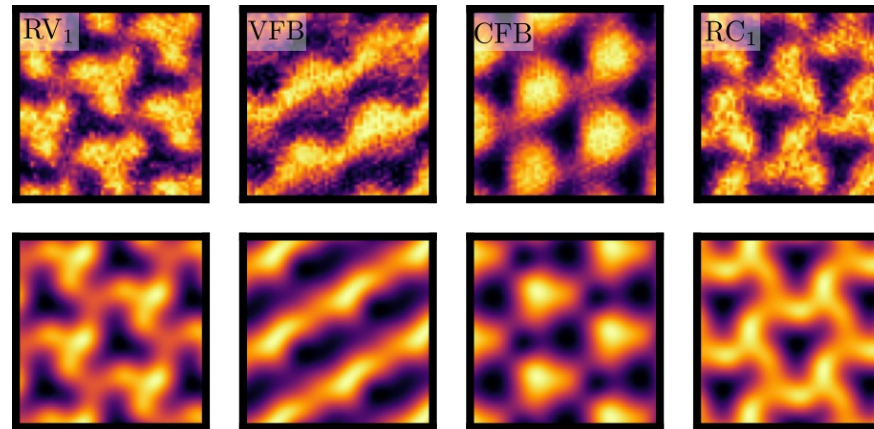


Machine Learning the Microscopic Form of Nematic Order in twisted double-bilayer graphene



João Augusto Sobral (University of Innsbruck -> University of Stuttgart)

Journal Club for Quantum Physics and Machine Learning (27/06/2023), ultracold.org

Acknowledgments



Simon Eli Turkel
Columbia University



Abhay Pasupathy
Columbia University



Stefan Obernauer
University of Innsbruck



Mathias S. Scheurer,
University of Innsbruck →
University of Stuttgart

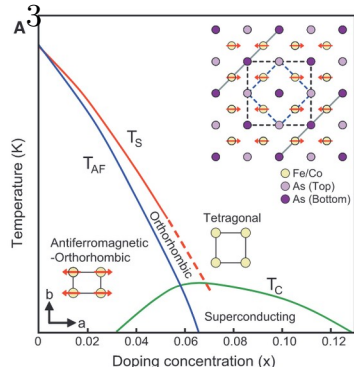
- Funding by the European Union (ERC-2021-STG, Project 101040651---SuperCorr).
- Discussions with Sayan Banerjee (UIBK), J. P. Valeriano (ICTP-SAIFR/Brazil), Igor Reis (USP/Brazil), Pedro H. P. Cintra (Unicamp/Brazil).
- More information about the slides: joaosds.github.io



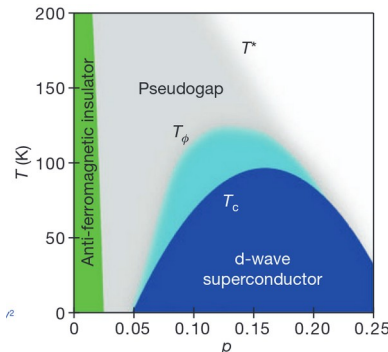
Funded by the
European Union

Nematicity

CaFe_2As_2
Iron-based superconductor

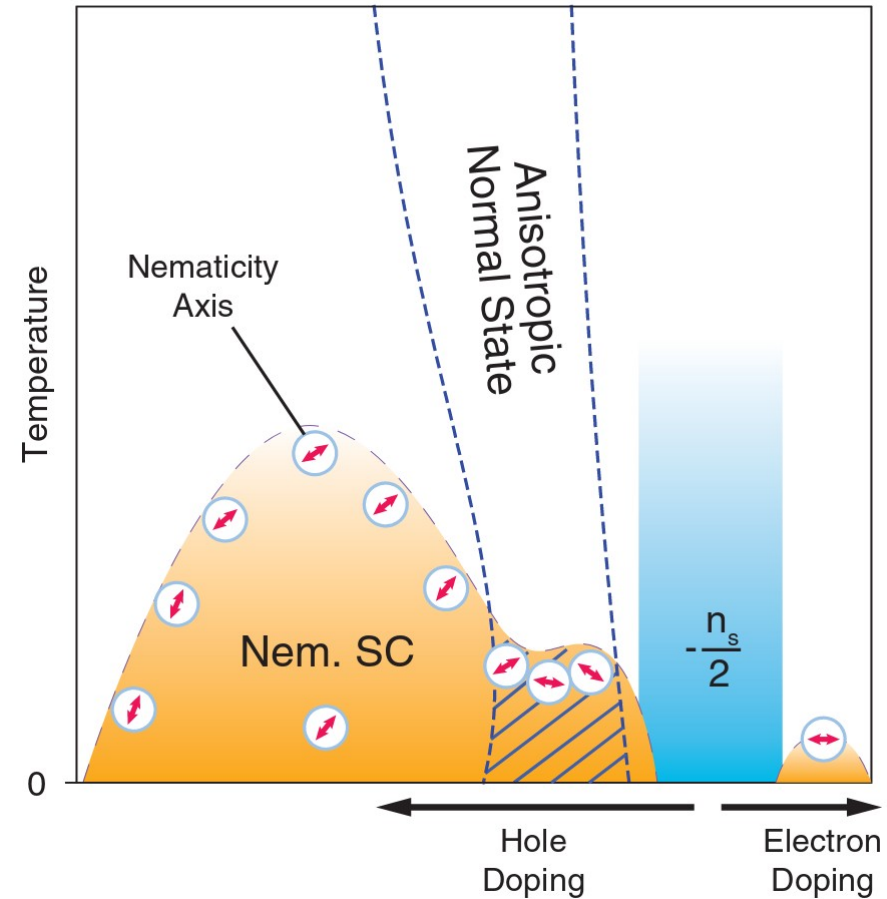


$\text{Bi}_2\text{Sr}_2\text{CaCu}_2\text{O}_{8+\delta}$
Copper-oxide superconductors

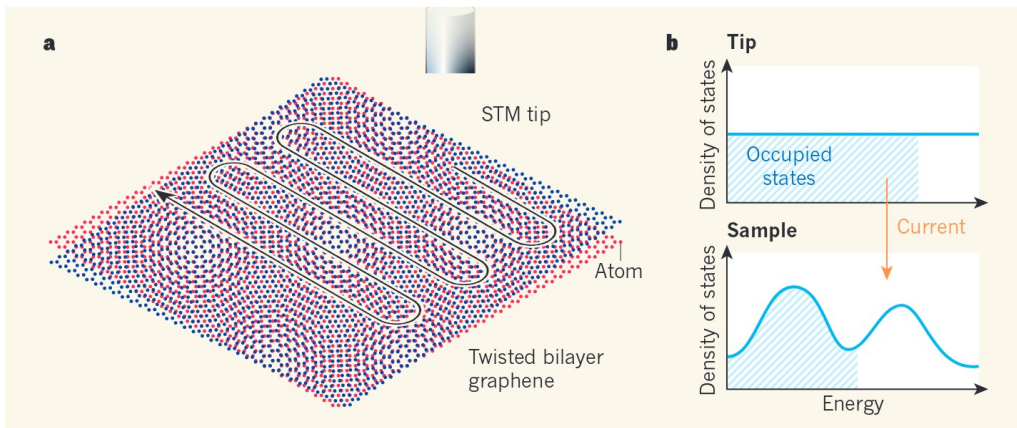


Lawler, M.J. et al, 2010. Nature, 466(7304) | Chuang, T.M, et al , 2010. Science, 327(5962), pp.181-184. | Fernandes, R.M., Chubukov, A.V. and Schmalian, J., 2014. Nature physics, 10(2), pp.97-104.

TBG: Y. Cao, D. Rodan-Legrain, J. M. Park, N. F. Q. Yuan, K. Watanabe, T. Taniguchi, R. M. Fernandes, L. Fu, and P. Jarillo-Herrero. Science 372, 264 (2021)

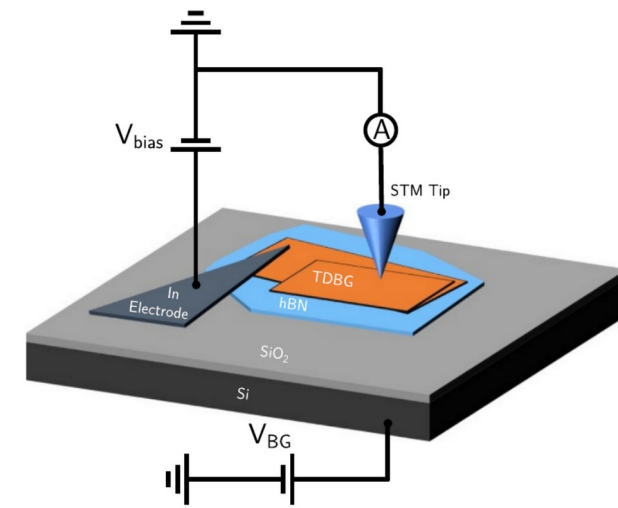
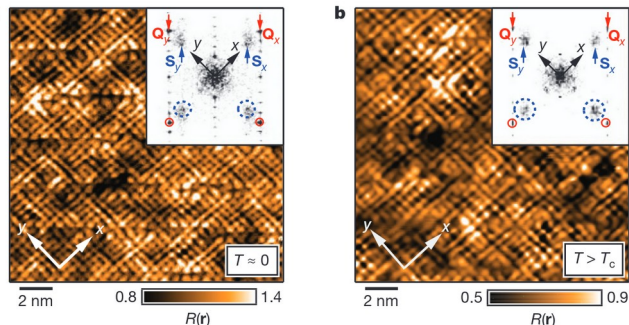


STM

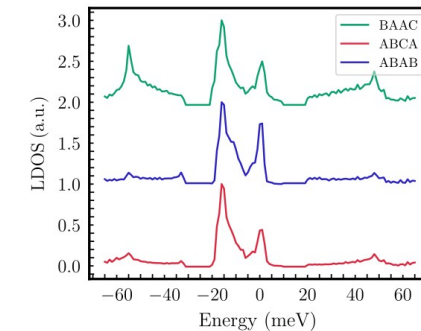
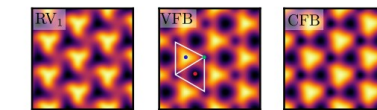


Scheurer, M.S., 2019. Spectroscopy of graphene with a magic twist. Nature, 572(7767), pp.40-41.

$$dI/dV \propto \mathcal{D}(\mathbf{r}, E)$$



R. Samajdar, M. S. Scheurer, S. Turkel, et al. 2D Materials 8, 034005 (2021).

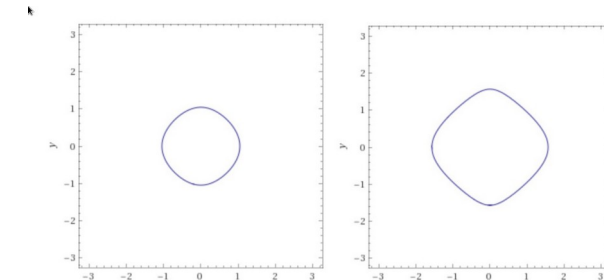
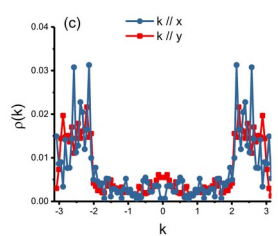
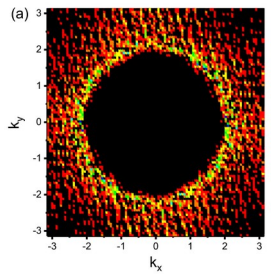


Using AI to detect nematicity

$$H = H_0 + H_{imp}$$

$$H_0 = - \sum_{\mathbf{r}} t_x c_{\mathbf{r}+\hat{x}}^\dagger c_{\mathbf{r}} + t_y c_{\mathbf{r}+\hat{y}}^\dagger c_{\mathbf{r}} + \text{h.c.}$$

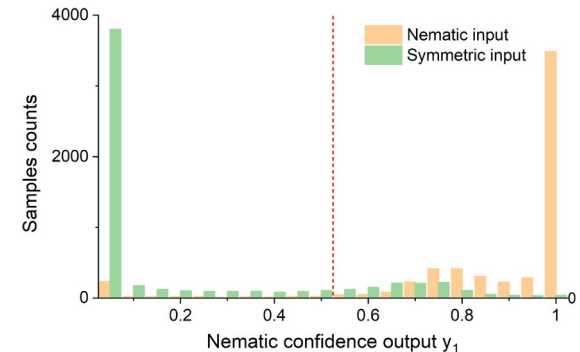
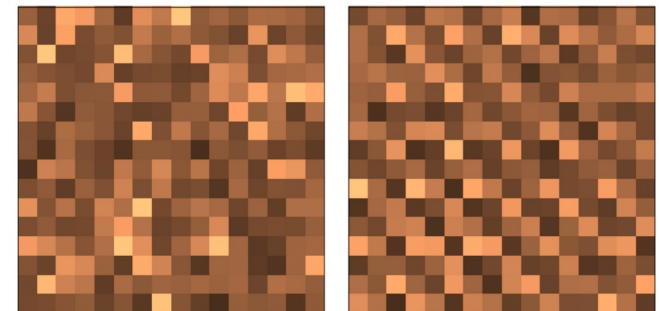
$$H_{imp} = \sum_{\mathbf{r} \in R_w} w_{\mathbf{r}} c_{\mathbf{r}}^\dagger c_{\mathbf{r}},$$



Goetz, J.B., et al 2020. SciPost Physics, 8(6), p.087.

$$O_N = \sum_{\mathbf{r}} N_{\mathbf{r}} [\underbrace{\cos(\mathbf{Q}_x \cdot \mathbf{r}) - \cos(\mathbf{Q}_y \cdot \mathbf{r})}_{\text{DOS}}]$$

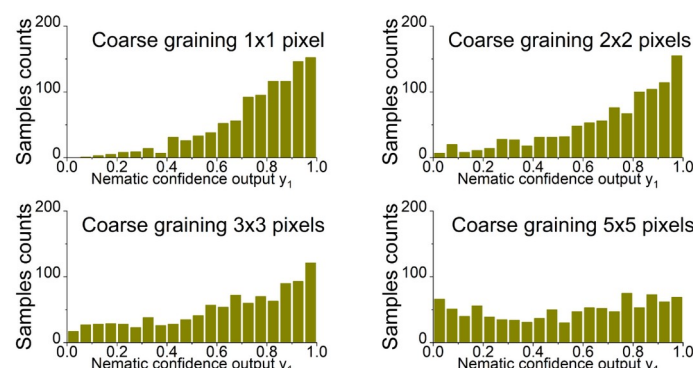
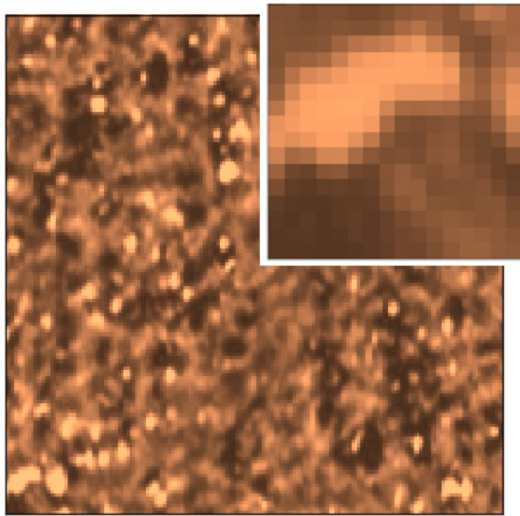
$$\mathbf{Q}_x = \left(\frac{2\pi}{a}, 0 \right) \text{ and } \mathbf{Q}_y = \left(0, \frac{2\pi}{a} \right)$$



Using AI to detect nematicity

CaFe₂As₂

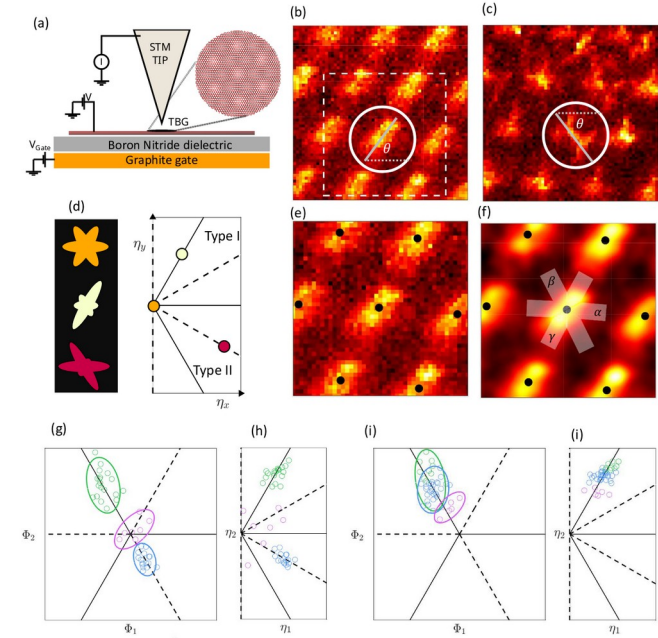
Goetz, J.B., et al 2020. SciPost Physics, 8(6), p.087.



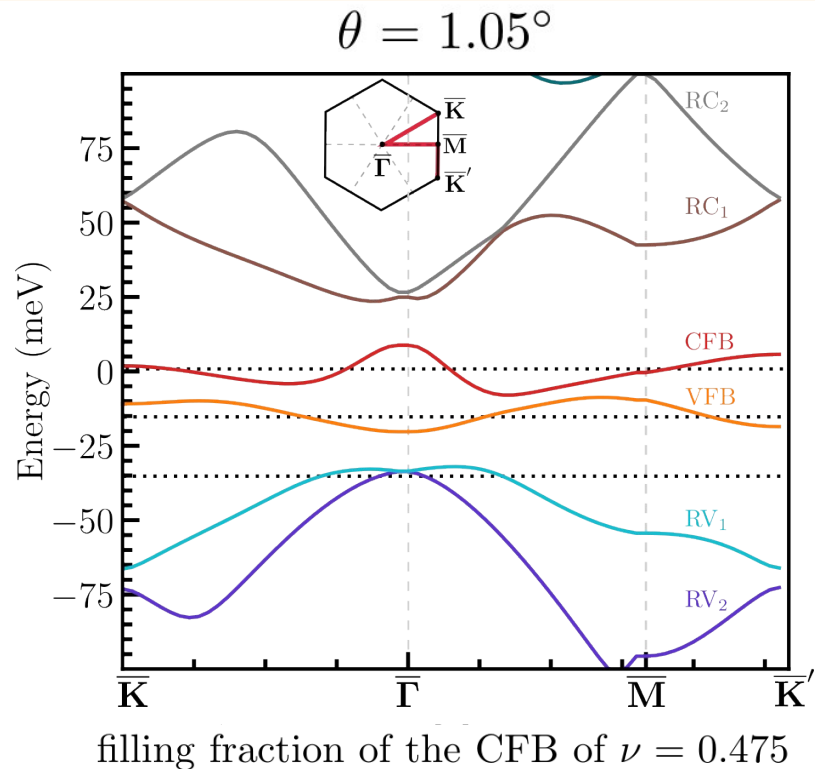
- ~90% exp dataset nematic;
- Need at least one hidden layer - \rightarrow Non linearity...;
- Disorder in TB model is needed;
- No microscopic form;

Nematicity in TBG

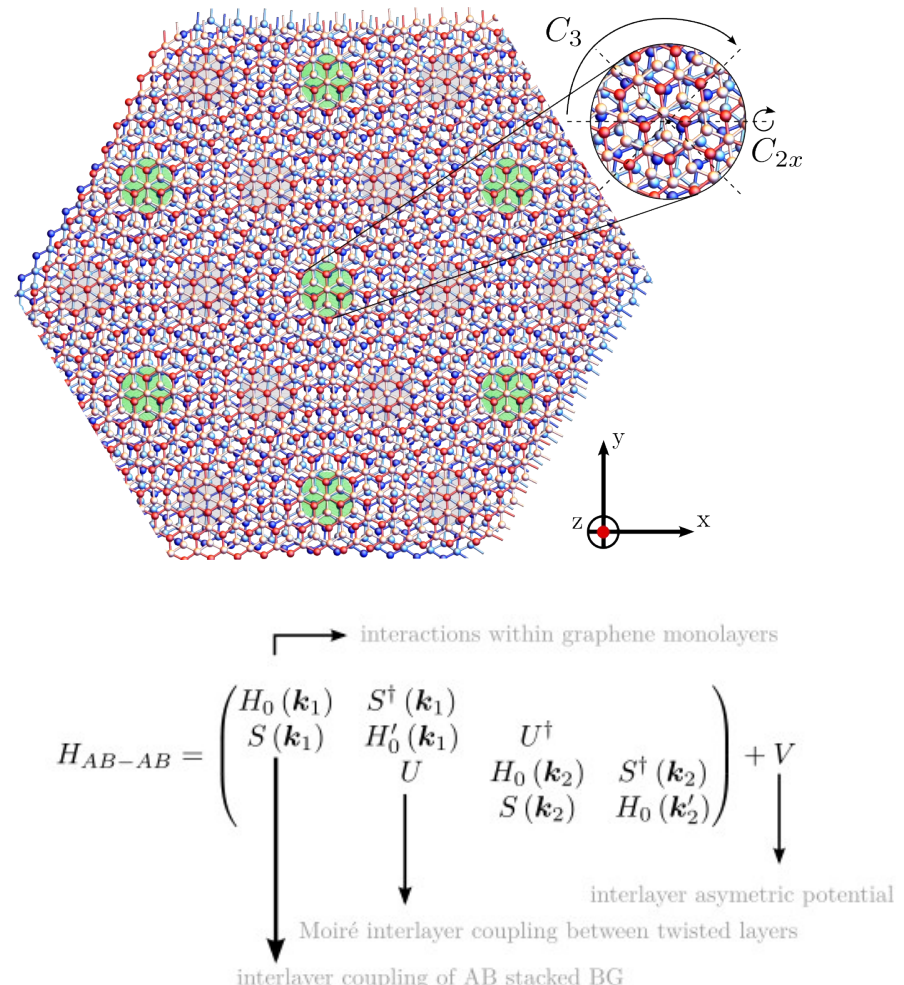
Taranto, W., et al 2022. arXiv preprint arXiv:2203.04449.



Twisted double-bilayer graphene (TDBG)

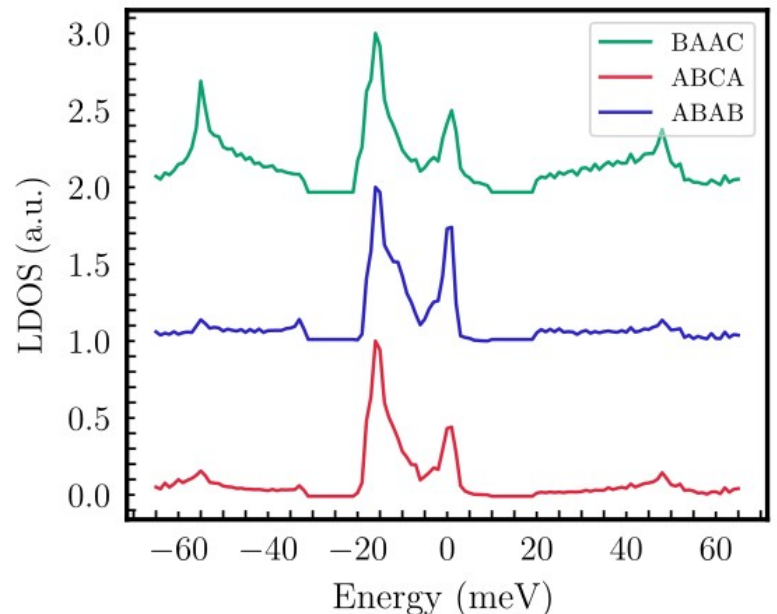
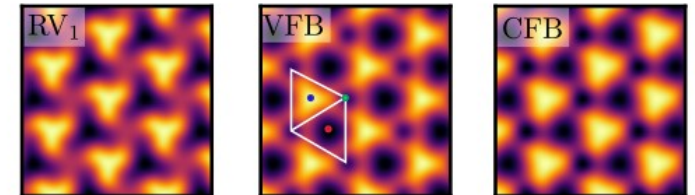


- Stiffness of bilayer graphene \rightarrow uniform samples, low strain.

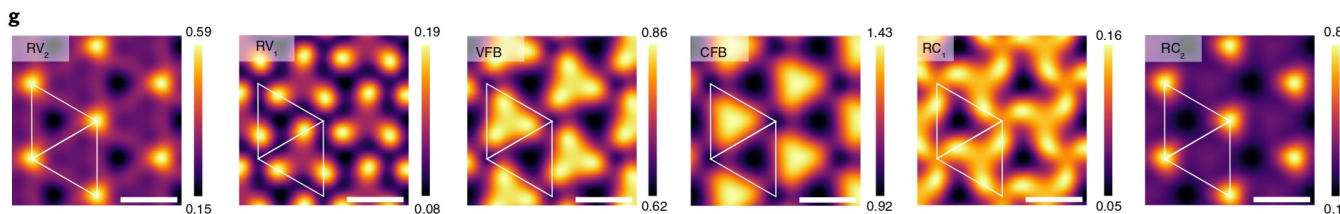
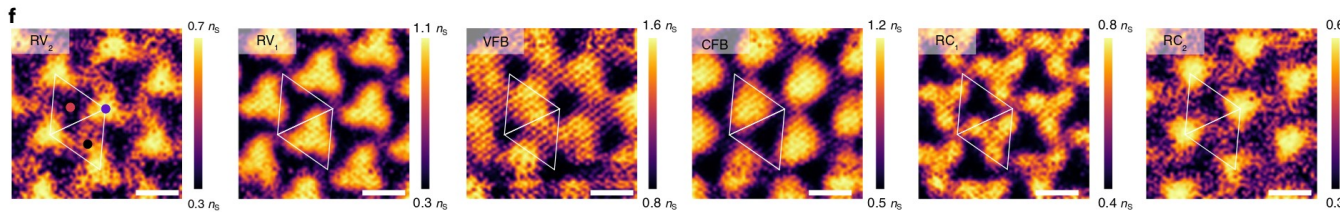
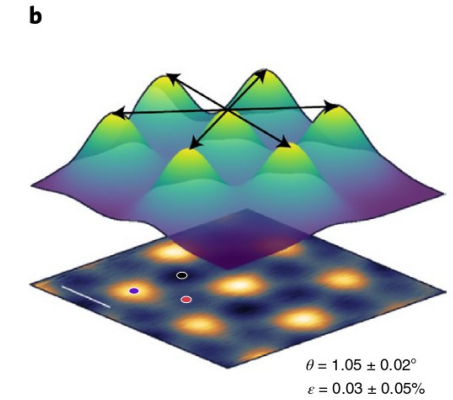
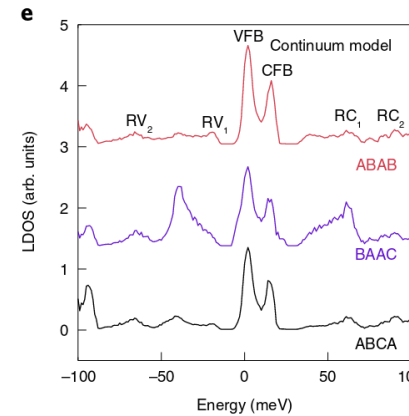
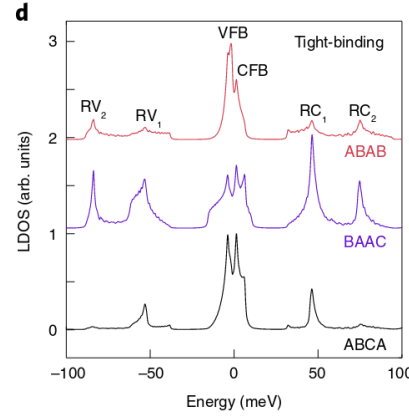
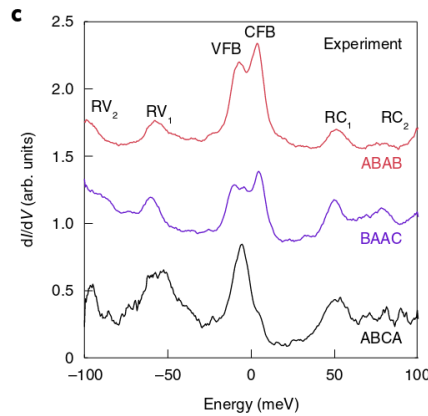


Local Density of States (LDOS)

$$\begin{aligned}\mathcal{D}(\mathbf{r}, E) &= \\ &= \sum_{n,\mathbf{k}} \sum_{\mathbf{G}, \mathbf{G}'} e^{-i(\mathbf{G}-\mathbf{G}') \cdot \mathbf{r}} \delta(E - E_{n,\mathbf{k}}) \\ &\quad \times \left(\left[U_{n,\mathbf{k}}^{A_4}(\mathbf{G}') \right]^* U_{n,\mathbf{k}}^{A_4}(\mathbf{G}) \right. \\ &\quad \left. + \left[U_{n,\mathbf{k}}^{B_4}(\mathbf{G}') \right]^* U_{n,\mathbf{k}}^{B_4}(\mathbf{G}) \right) \\ &\quad \text{(LDOS) projected onto} \\ &\quad \text{4th graphene layer}\end{aligned}$$



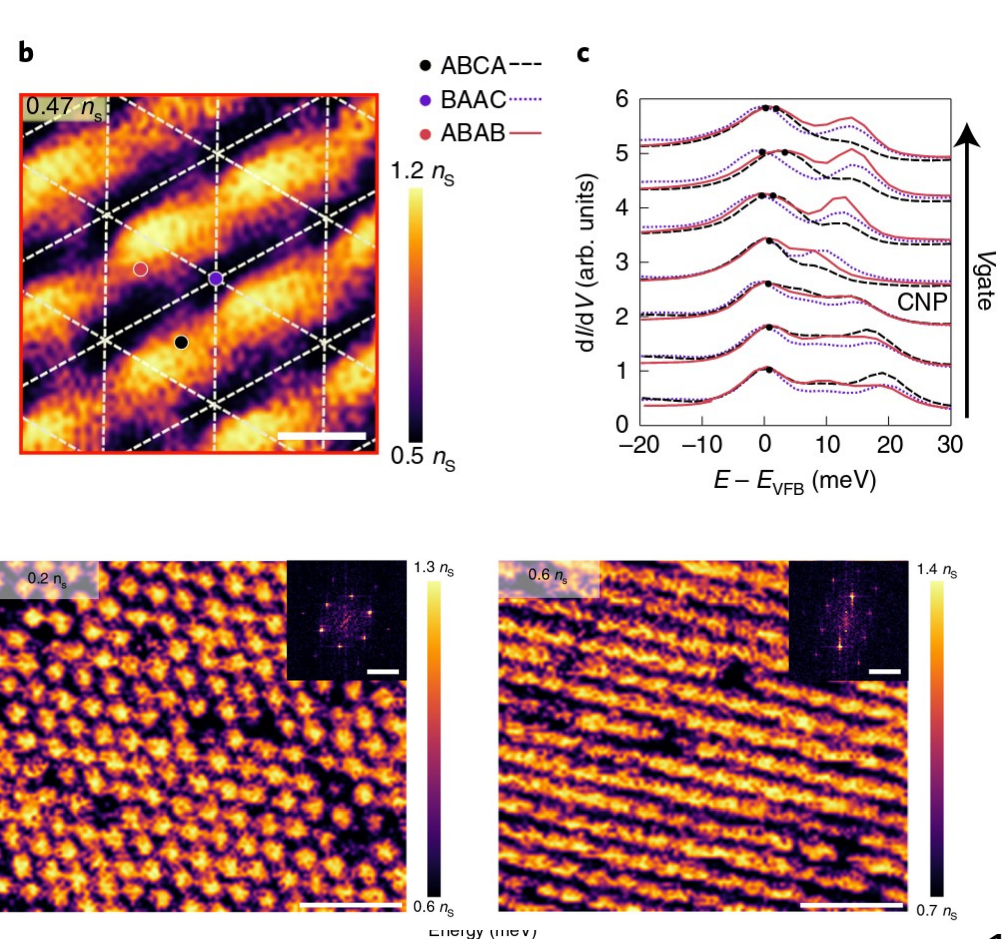
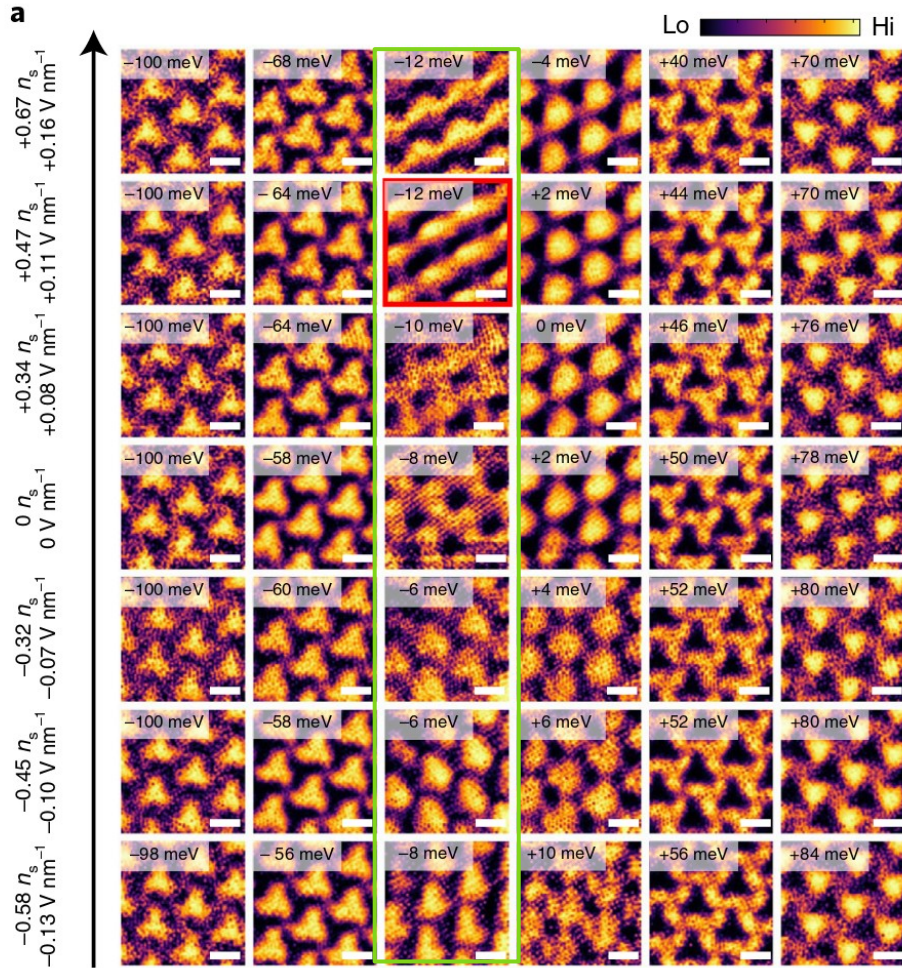
Nematicity in TDBG



● ABAB ● BAAC ● ABCA

Rubio-Verdú, C., et al, 2022. Nature Physics, 18(2), pp.196-202. | R. Samajdar, M. S. Scheurer, S. Turkel, et al. 2D Materials 8, 034005 (2021).

Nematicity in TDBG



Nematicity in TDBG

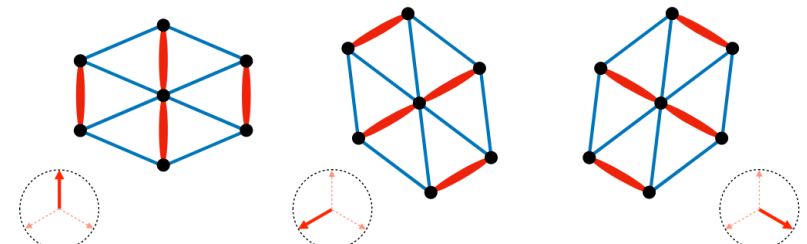
spin, layer, sublattice and valley degrees of freedom

$$\mathcal{H}_\Phi = \int_{\mathbf{r}} \int_{\Delta \mathbf{r}} \Phi \cdot \phi_{\ell,s,\eta;\ell',s',\eta'}(\mathbf{r}, \Delta \mathbf{r}) c_{\sigma,\ell,s,\eta}^\dagger(\mathbf{r} + \Delta \mathbf{r}) c_{\sigma,\ell',s',\eta'}(\mathbf{r}) + \text{H.c.}$$

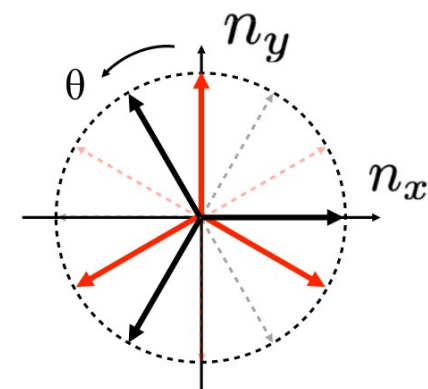
$$\Phi = \Phi (\cos 2\varphi, \sin 2\varphi)$$

intensity

nematic director angle



- Graphene nematicity (GN);
- Moiré Nematicity (MN);



R. Samajdar, M. S. Scheurer, S. Turkel, et al. 2D Materials 8, 034005 (2021).

Moiré Nematicity (MN)

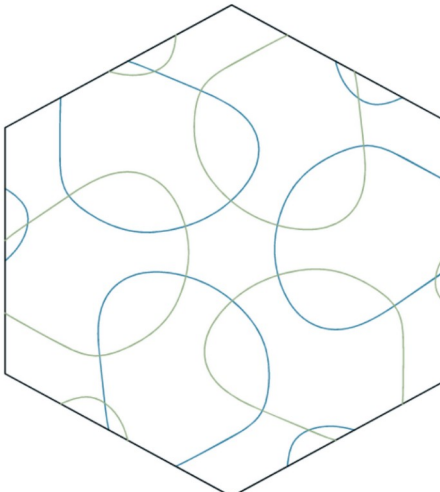
$$\mathcal{H}_{\Phi}^{MN} = \Phi \cdot \mathbf{f}(\mathbf{k}) c_{\alpha}^{\dagger}(\mathbf{k}) c_{\alpha}(\mathbf{k})$$

$$E_{n,\mathbf{k}} \rightarrow E_{n,\mathbf{k}} + \Phi \cdot \mathbf{f}(\mathbf{k}),$$

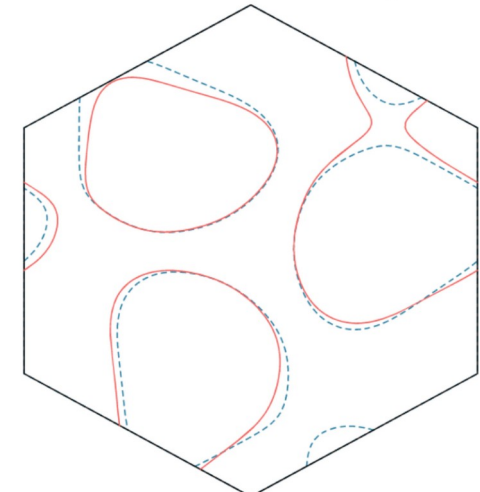
$$\mathbf{f}(\mathbf{k}) = \sum_{m_1, m_2 \in \mathbb{Z}} \phi_{m_1, m_2} \cos(\mathbf{k} \cdot \mathbf{R}_{m_1, m_2})$$

Transforms as E irred. of D_3

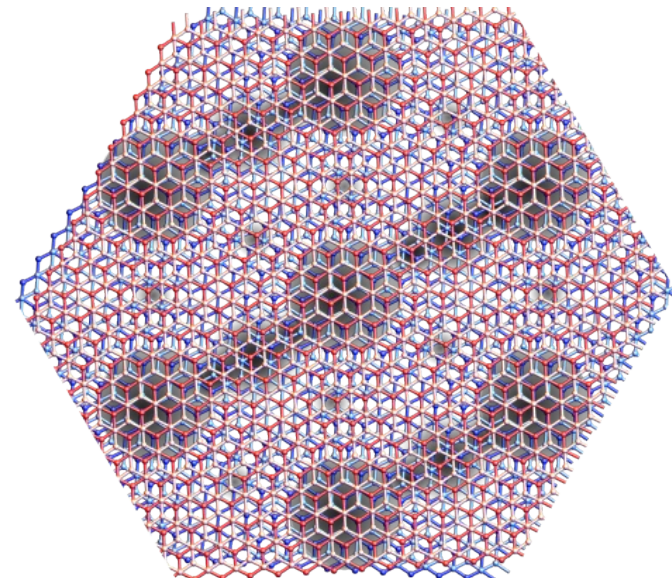
C_3 symmetric



Moiré Nematicity



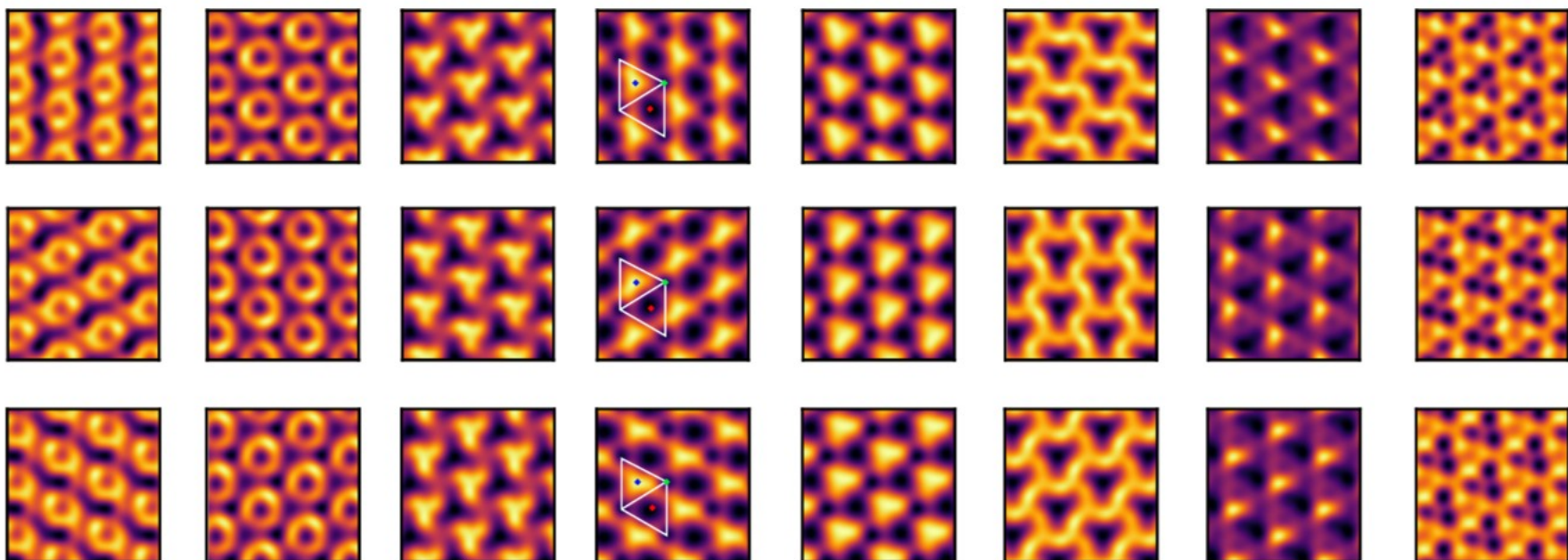
- Stronger effects close to van-Hove singularities
- Breaks C_3 symmetry at moiré scale.
- Learnable parameters: φ_{MN} and Φ_{MN} .



Moiré Nematicity (MN)

Moiré Nematicity (MN) $\boxed{\Phi = 5 \text{ meV}}$

-85 meV (RV₂) -66 meV (RV₂) -37 meV (RV₁) -15 meV (VFB) +1 meV (CFB) +24 meV (RC₁) +66 meV (RC₂) +77 meV (RC₂)



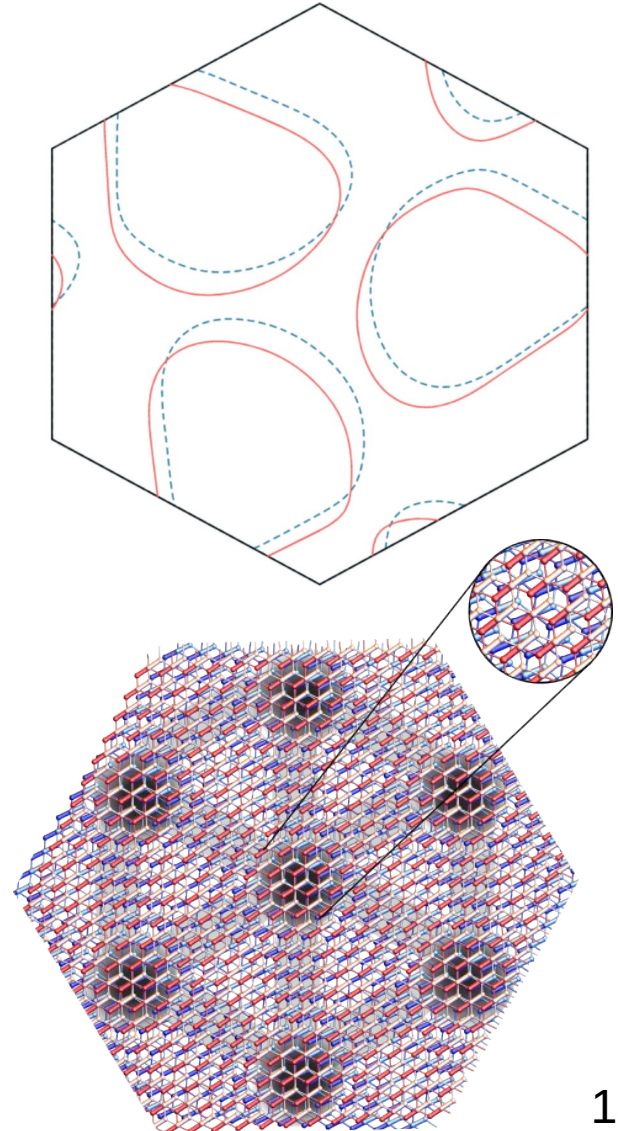
Graphene nematicity (GN)

$$\phi_{l,s; l', s'} (\eta) = \delta_{l,l'} \psi_l \left(\frac{(e^{i\alpha_l \eta \rho_z} \rho_x)_{ss'}}{\eta (e^{i\alpha_l \eta \rho_z} \rho_y)_{ss'}} \right), \quad \psi_l, \alpha_l \in \mathbb{R}.$$

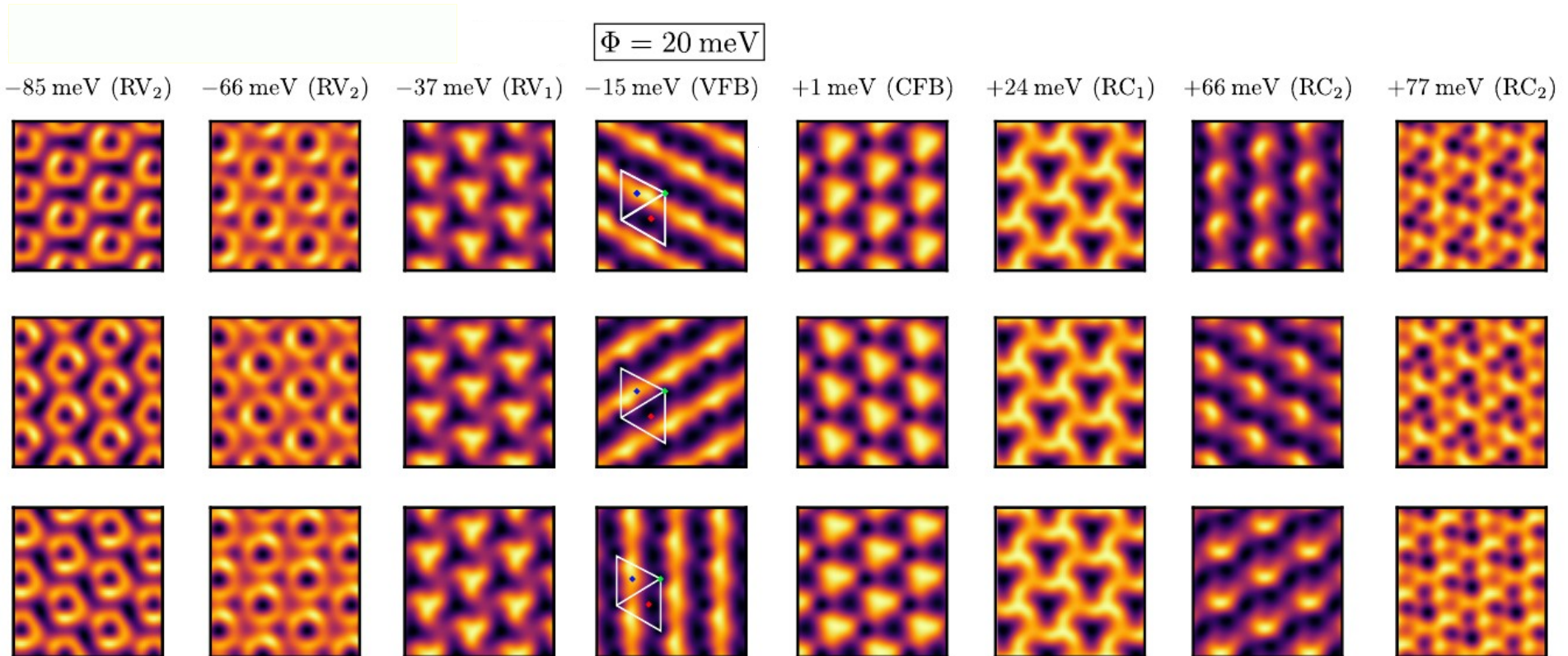
$$H_0(\mathbf{k}) \rightarrow H_0(\mathbf{k}) + \Phi \cdot \phi_{s,s'} = \\ = \begin{pmatrix} 0 & -\hbar\nu k_- + \Phi \cdot M_\alpha \\ -\hbar\nu k_+ + \Phi \cdot M_\alpha^\dagger & d \end{pmatrix} \quad M_{\alpha_l} = (1, -i\eta) e^{i\alpha_l \eta}.$$

$$\mathcal{H}_l = -\hbar\nu \left[R(\pm\theta/2) \left(\mathbf{k} - \mathbf{K}_\eta^l \right) \right] \cdot (\eta \rho_x, \rho_y) + \boxed{\Phi \cdot (\rho_x, \eta \rho_y)}$$

- Shifts Dirac cones.
- Breaks C3 symmetry at atomic scale;
- Learnable parameters: $\varphi_{GN}, \Phi_{GN}, \alpha, \dots$

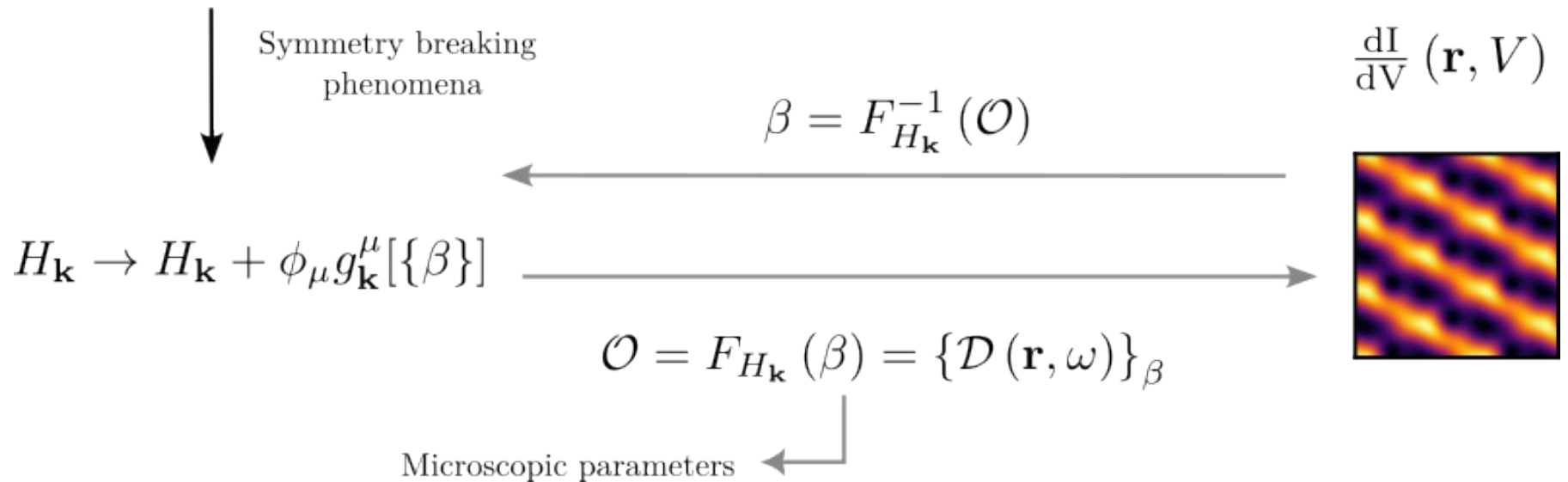


Graphene nematicity (GN)



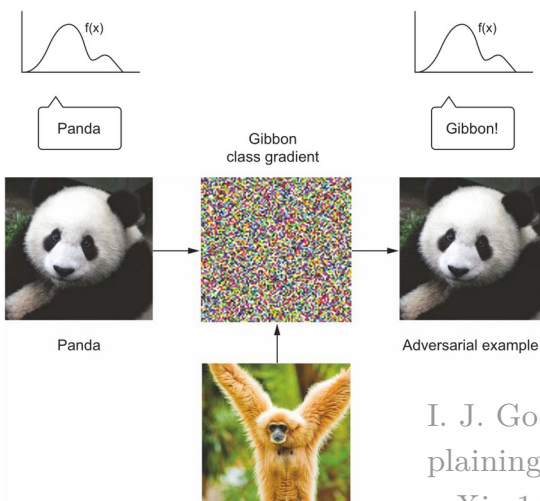
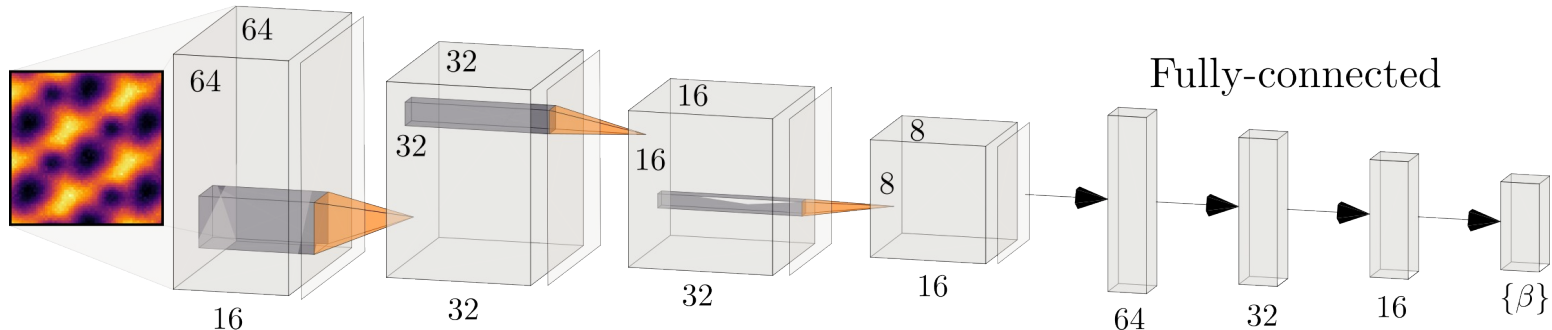
Solving the Inverse Problem

$$H_{\mathbf{k}} = H_{\mathbf{k}} [t_j]$$

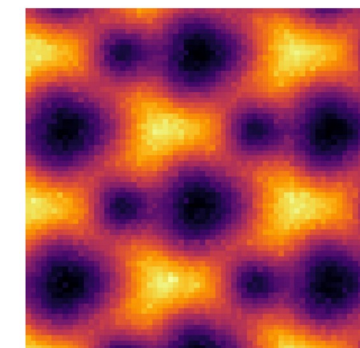


DL Architecture

Convolution and max pooling

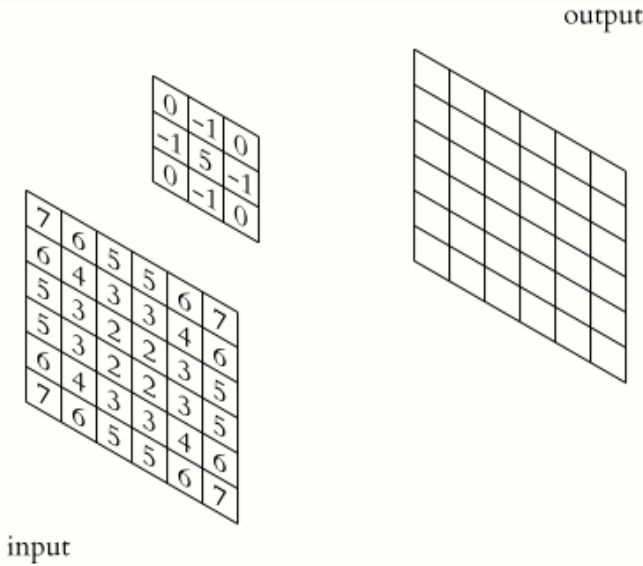


$$p_g(z) = \frac{\exp(-(z-\mu)^2/2\sigma^2)}{\sqrt{2\pi}\sigma^2}$$
$$\sigma \approx 0.31, \mu = 0$$



I. J. Goodfellow, J. Shlens, and C. Szegedy, “Explaining and Harnessing Adversarial Examples,” (2015), arXiv:1412.6572 [cs, stat].

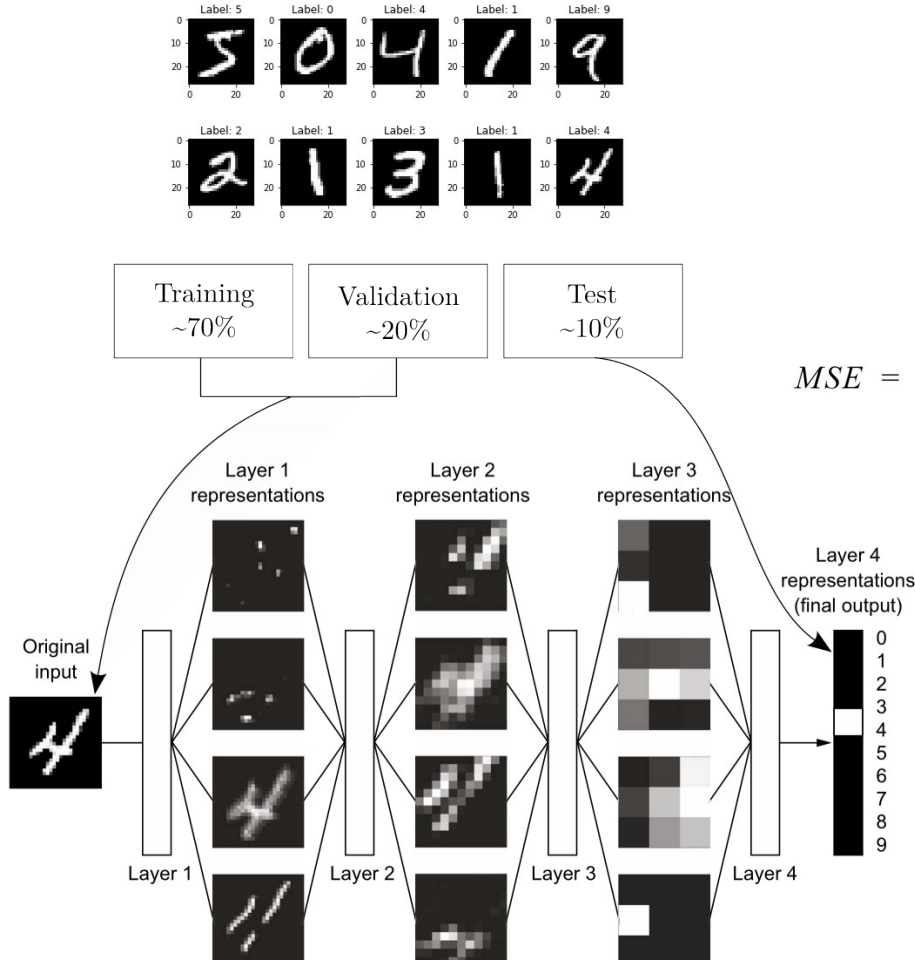
CNN's learning procedure



input

@[https://en.wikipedia.org/wiki/Kernel_\(image_processing\)](https://en.wikipedia.org/wiki/Kernel_(image_processing))

Operation	Kernel ω	Image result $g(x,y)$
Identity	$\begin{bmatrix} 0 & 0 & 0 \\ 0 & 1 & 0 \\ 0 & 0 & 0 \end{bmatrix}$	
Ridge detection	$\begin{bmatrix} -1 & -1 & -1 \\ -1 & 4 & -1 \\ -1 & -1 & -1 \end{bmatrix}$	
	$\begin{bmatrix} -1 & -1 & -1 \\ -1 & 8 & -1 \\ -1 & -1 & -1 \end{bmatrix}$	

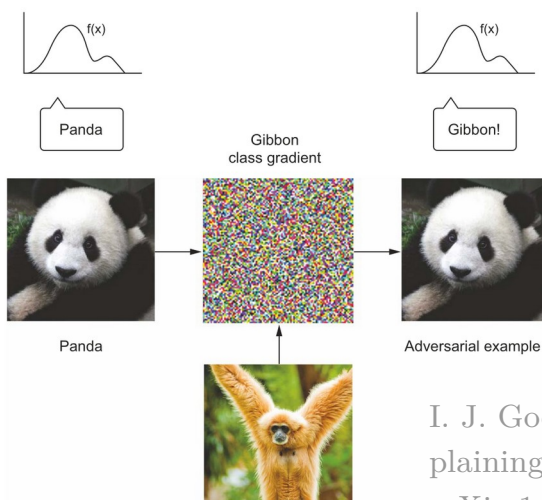
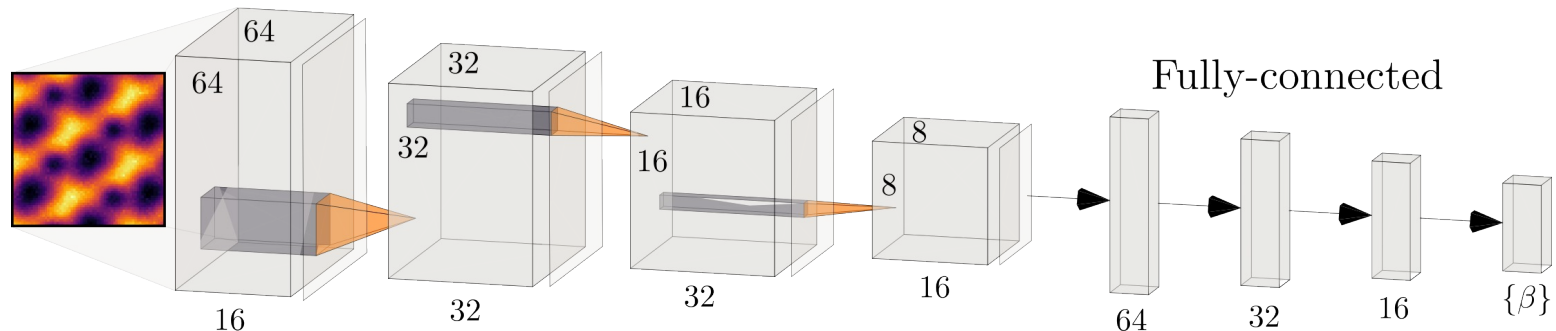


$$MSE = \frac{1}{n} \sum \left(y - \hat{y} \right)^2$$

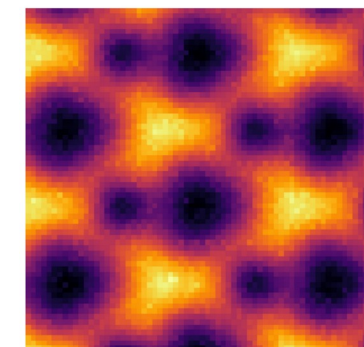
The square of the difference between actual and predicted

DL Architecture

Convolution and max pooling



$$p_g(z) = \frac{\exp(-(z-\mu)^2/2\sigma^2)}{\sqrt{2\pi}\sigma^2}$$
$$\sigma \approx 0.31, \mu = 0$$



I. J. Goodfellow, J. Shlens, and C. Szegedy, “Explaining and Harnessing Adversarial Examples,” (2015), arXiv:1412.6572 [cs, stat].

Orientation of Nematic Director

intensity

$$\Phi = \Phi (\cos 2\varphi, \sin 2\varphi)$$

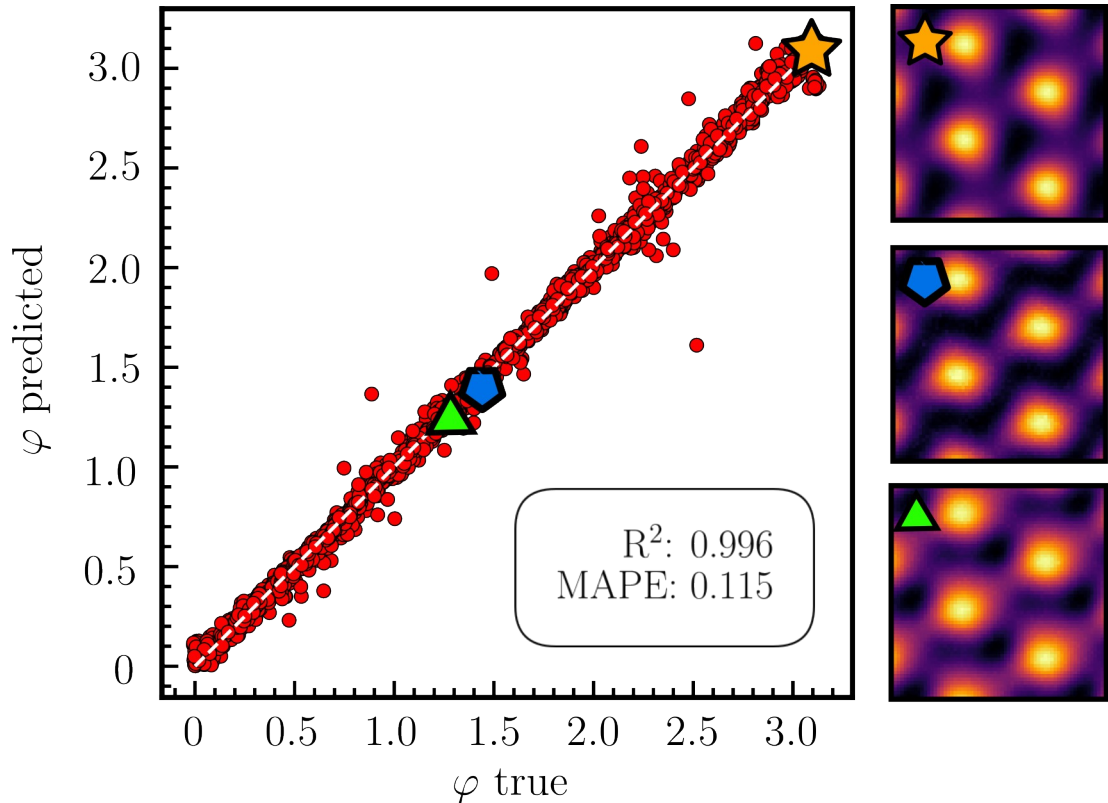
nematic director

angle

$$\varphi_i = \frac{1}{2} \arctan 2(\sin 2\varphi, \cos 2\varphi) \Rightarrow$$

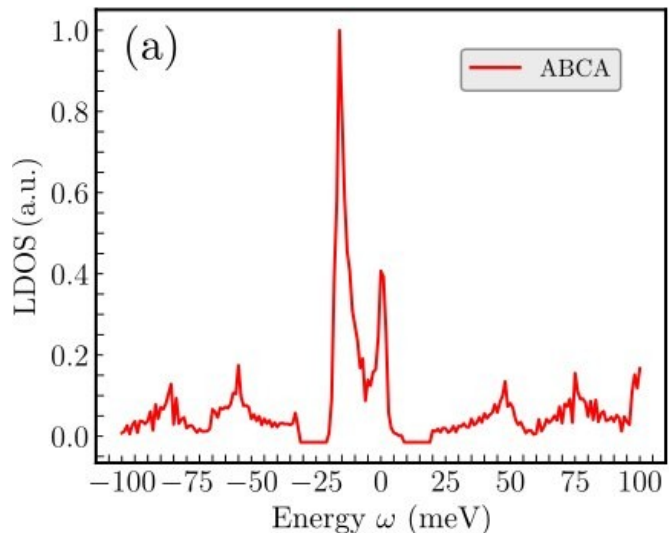
$$\Rightarrow \varphi = \begin{cases} \varphi_i, & \text{sgn}\varphi_i = 1 \\ \varphi_i + \pi, & \text{sgn}\varphi_i = -1 \end{cases}$$

→



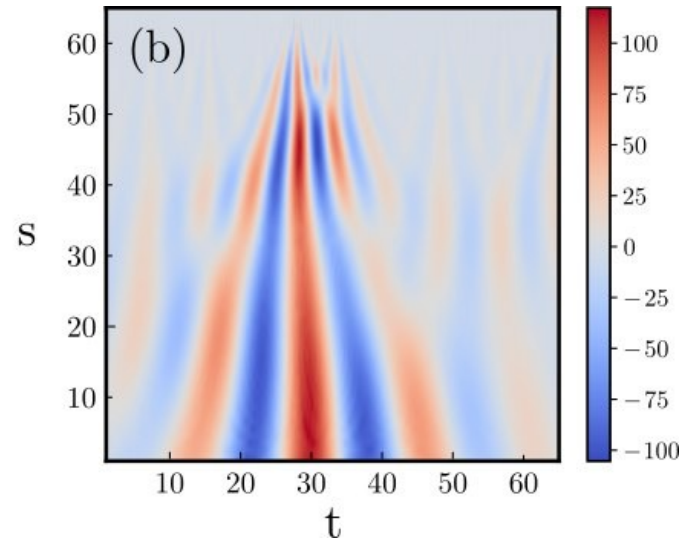
$$\mathcal{D}_{\text{th}} \rightarrow \phi_{\text{MN}}, \phi_{\text{GN}} \in [0.001, 0.1] \text{ eV}, \varphi = \varphi_{\text{MN}} = \varphi_{\text{GN}} \in [0, \pi]$$

More data: Adding $\mathcal{D}_{\mathbf{r}_0}(\omega)$ channels



CWT
→

with Morlet
wavelets

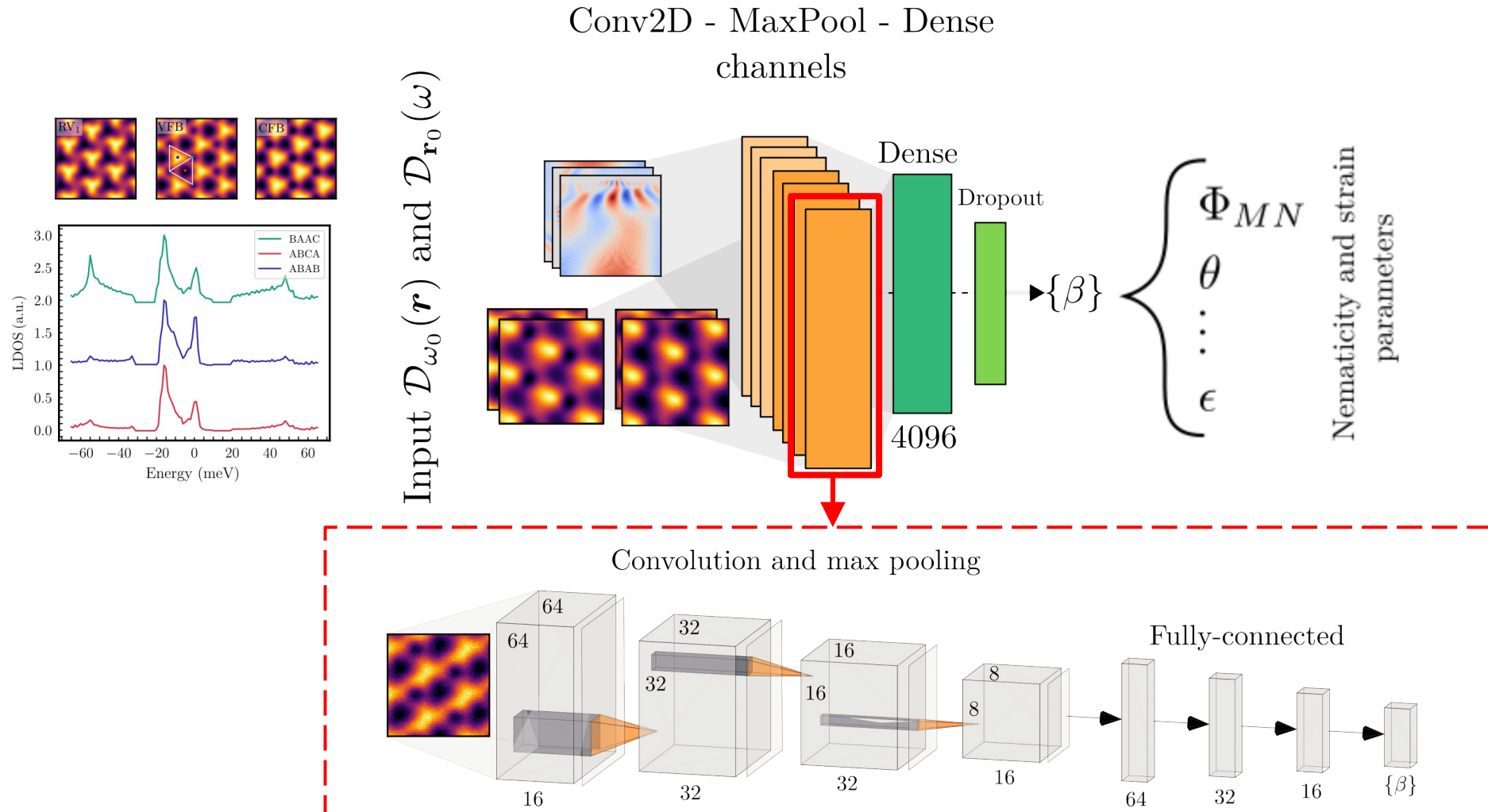


with gaussian noise

$$p_G(z) = \frac{1}{\sigma\sqrt{2\pi}} e^{-\frac{(z-\mu)^2}{2\sigma^2}}$$

$$\sigma = 0.31, \mu = \mathcal{D}(\omega)$$

New architecture



Back to the nematic microscopic form

$$E_{n,\mathbf{k}} \rightarrow E_{n,\mathbf{k}} + \Phi \cdot \mathbf{f}(\mathbf{k}),$$

$$\mathbf{f}(\mathbf{k}) = \sum_{m_1, m_2 \in \mathbb{Z}} \phi_{m_1, m_2} \cos(\mathbf{k} \cdot \mathbf{R}_{m_1, m_2})$$

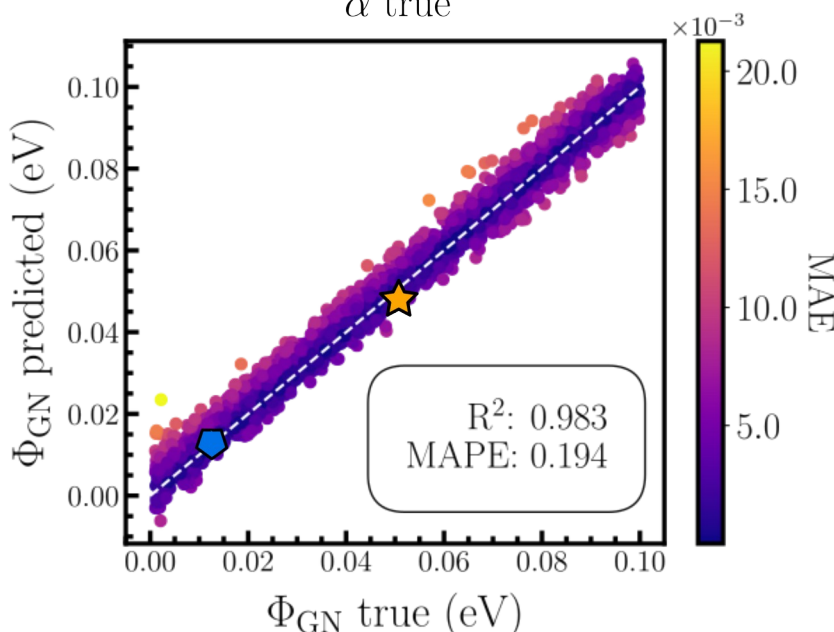
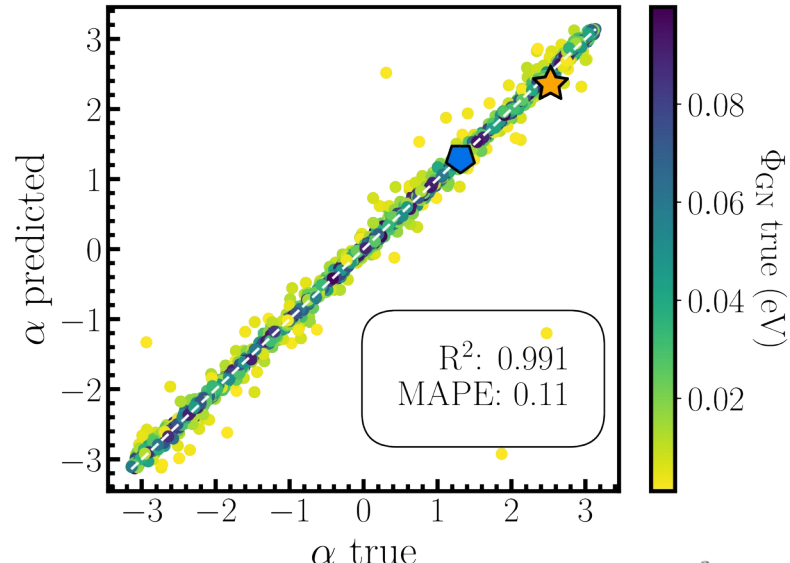
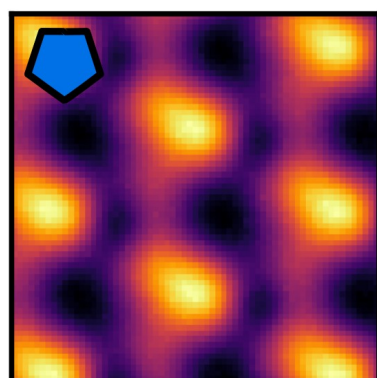
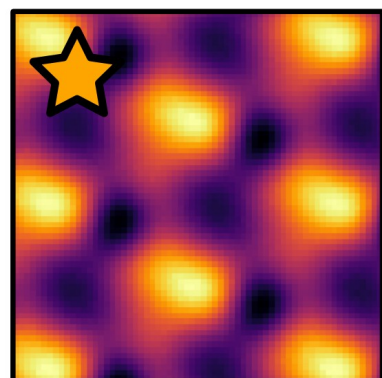
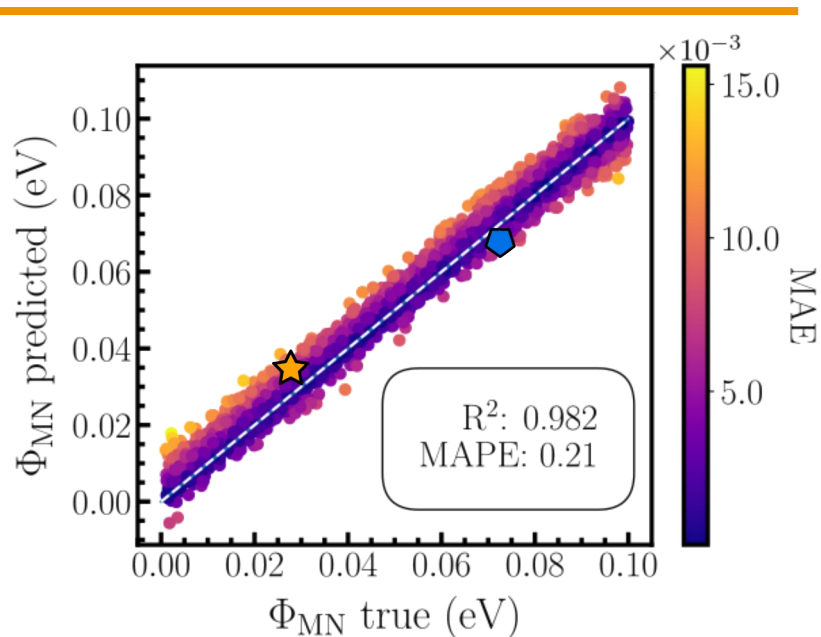
$$H_0(\mathbf{k}) \rightarrow H_0(\mathbf{k}) + \Phi \cdot \phi_{s,s'} = \begin{pmatrix} 0 & -\hbar\nu k_- + \Phi \cdot M_\alpha \\ -\hbar\nu k_+ + \Phi \cdot M_\alpha^\dagger & d \end{pmatrix}$$

$$M_{\alpha_l} = (1, -i\eta) e^{i\alpha_l \eta}.$$

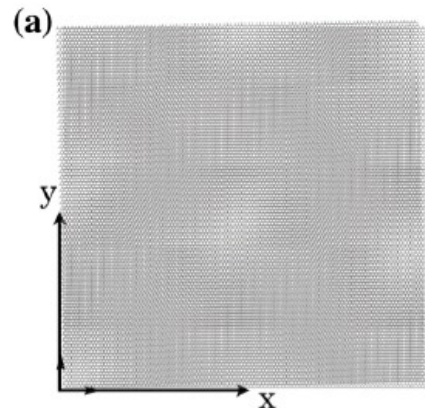
Learn

$$\beta = \{\Phi_{MN}, \Phi_{GN}, \alpha\}$$

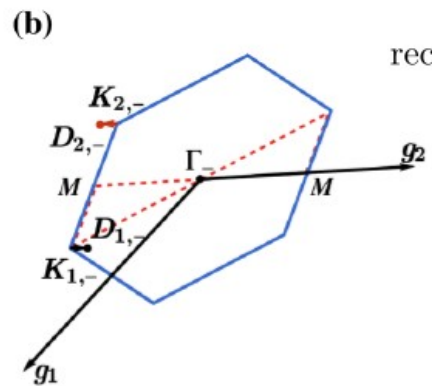
Form of nematicity



Including strain



(a)



(b)

moiré superlattice
reciprocal and primitive
latticevectors

small angle
rotation

$$\begin{cases} \mathbf{g}_i \cong \mathcal{E}^T \mathbf{G}_i \\ \mathbf{a}_i \cong \mathcal{E}^{-1} \mathbf{A}_i \end{cases}$$

monolayer graphene
reciprocal and primitive
latticevectors

learnable parameters

$$\mathcal{E} = \mathcal{T}(\theta) + S_{ua}(\overbrace{\varepsilon, \dot{\theta}_\varepsilon})$$

$$\mathcal{E} = \frac{1}{2} R(\theta_\epsilon)^{-1} \begin{pmatrix} -\epsilon & 0 \\ 0 & \nu\epsilon \end{pmatrix} R(\theta_\epsilon)$$

uniaxial strain

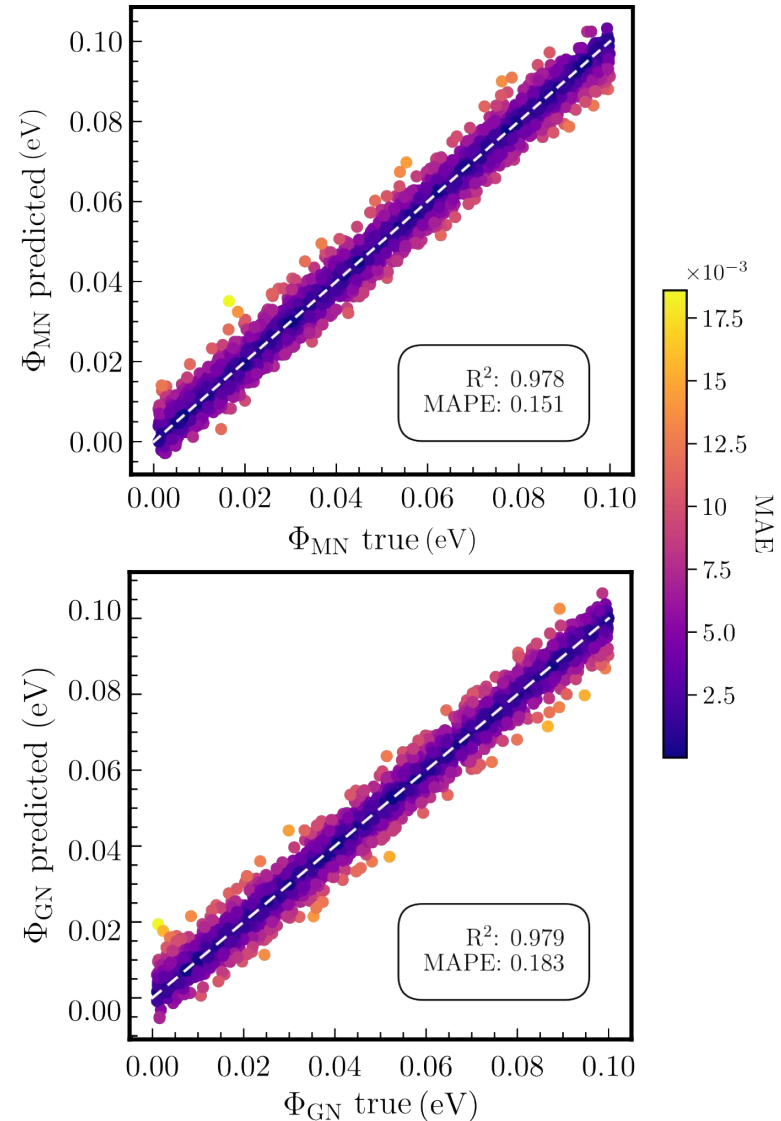
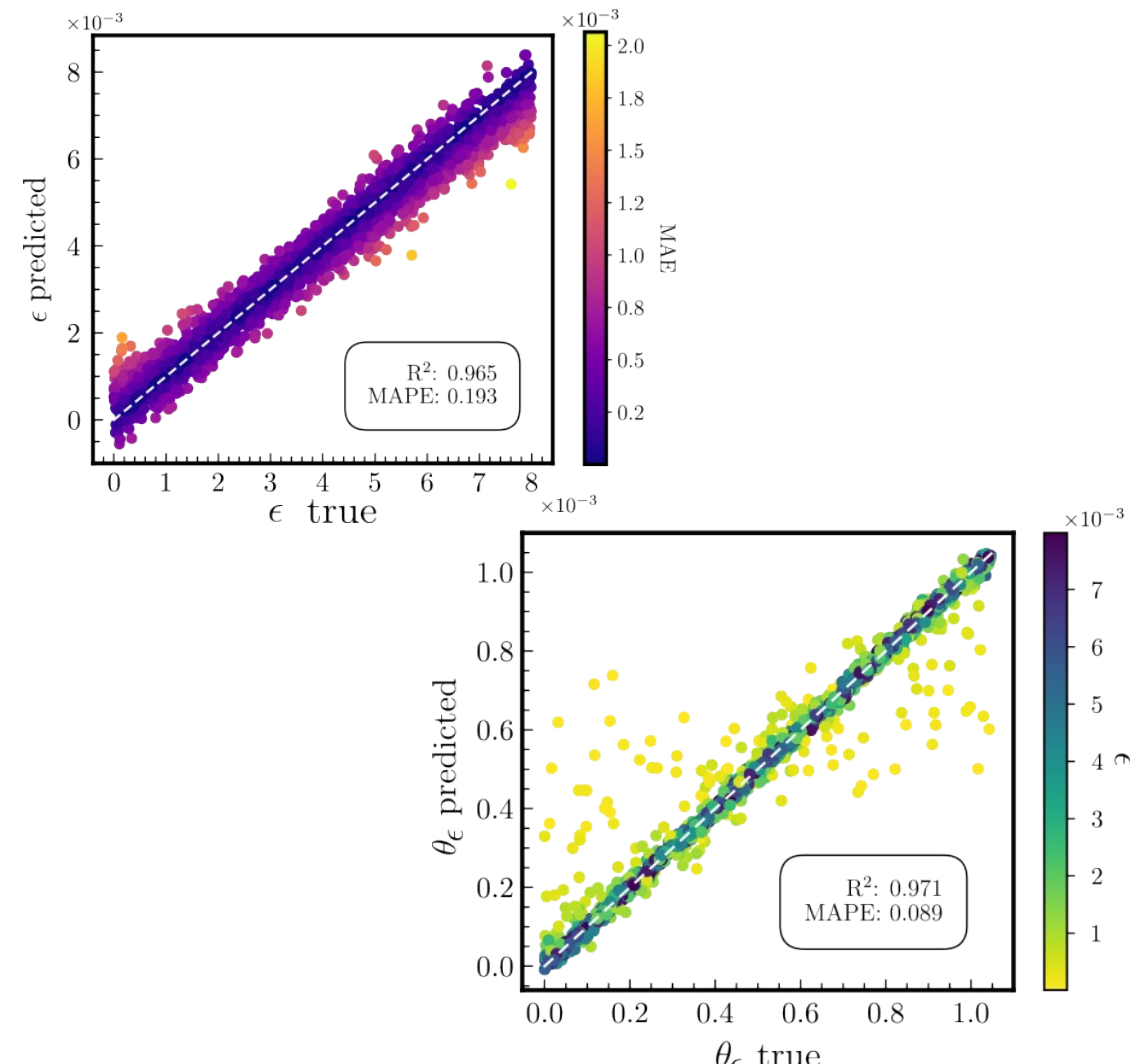
Fig. 1: Modification of Moiré Structure and Brillouin Zone with $\epsilon = 0.7\%$, $\varphi = 0^\circ$ and $\theta = 1.05^\circ$ [5].

Bi, Z., Yuan, N.F. and Fu, L., 2019. Physical Review B, 100(3), p.035448.

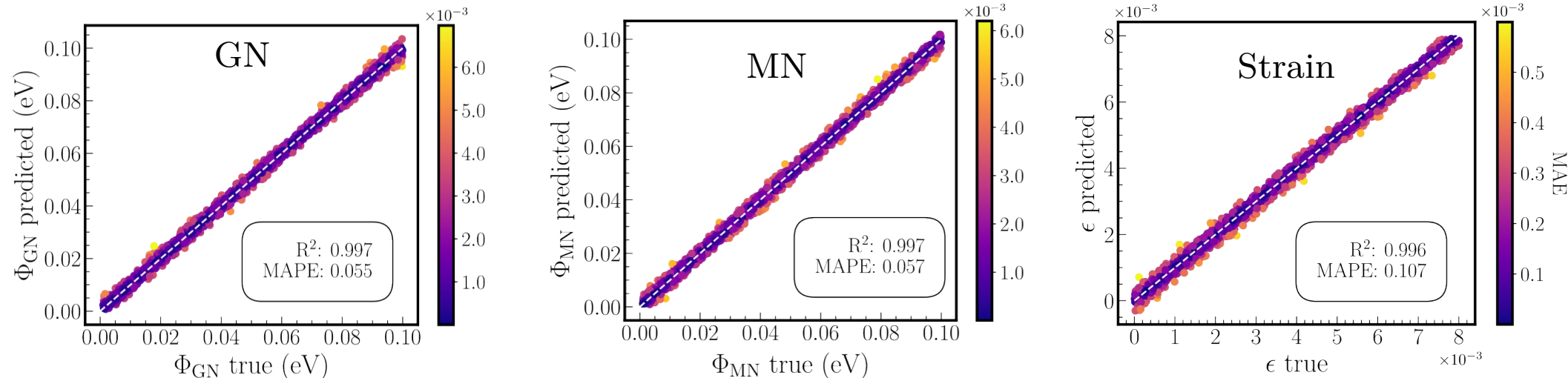
Learn

$\Phi_{MN}, \Phi_{GN}, \theta_\varepsilon, \epsilon$

Including strain

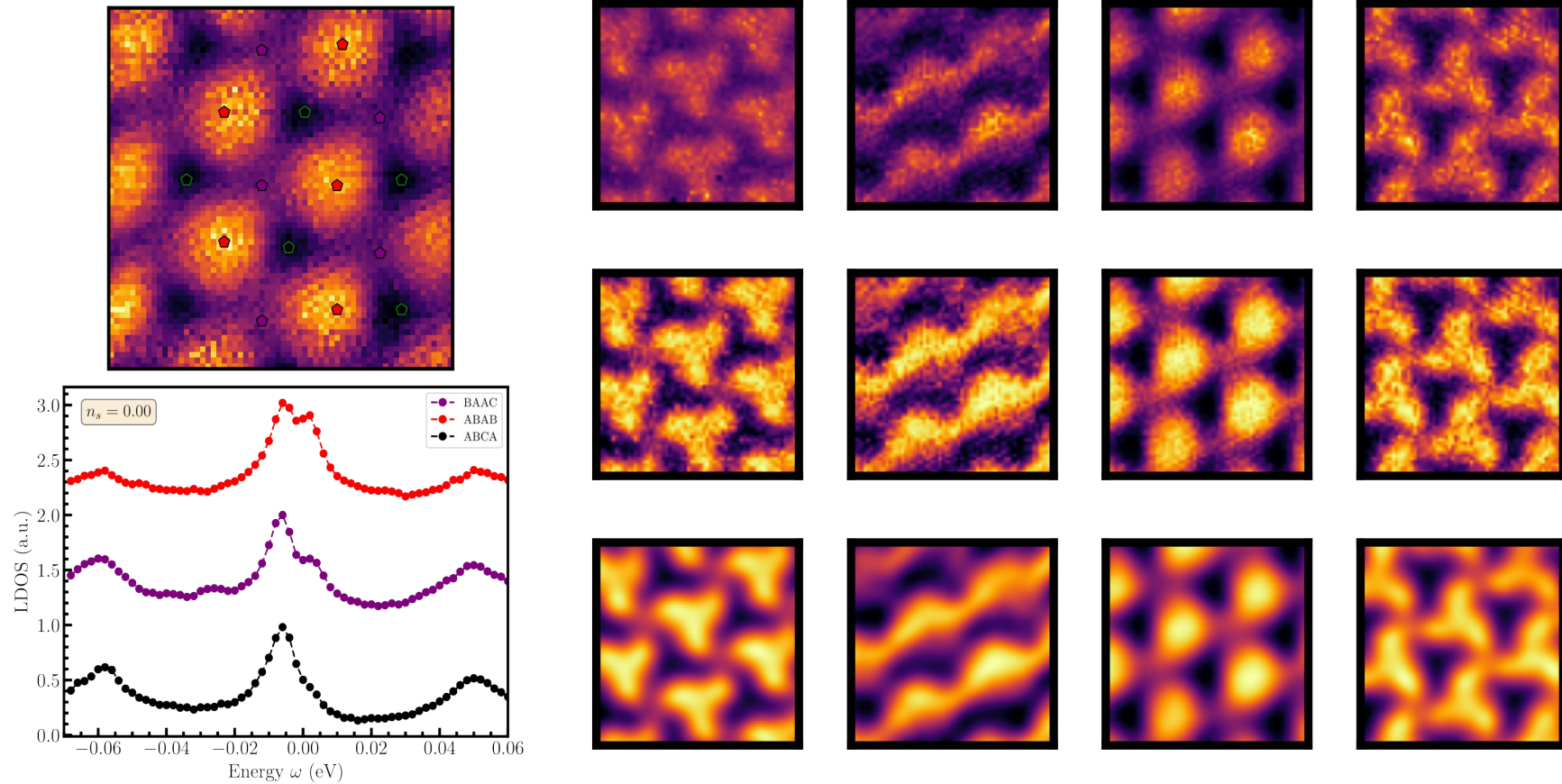


Including strain, fixed θ_ε

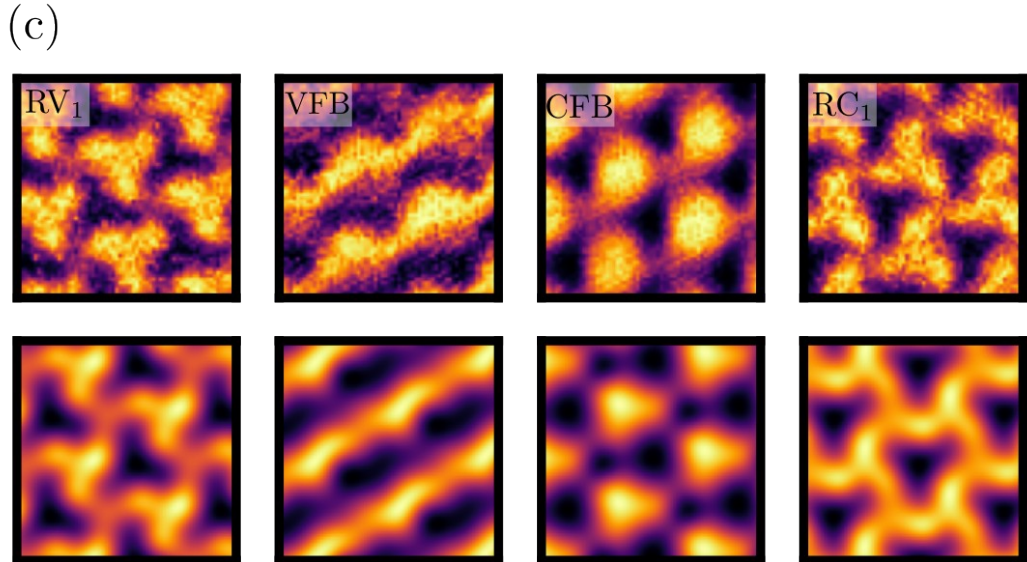
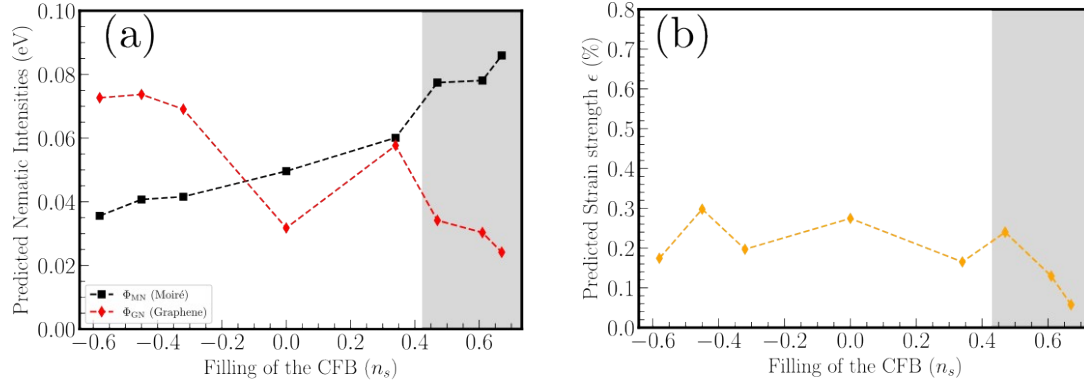


- Can we apply the trained CNN directly to experimental data?

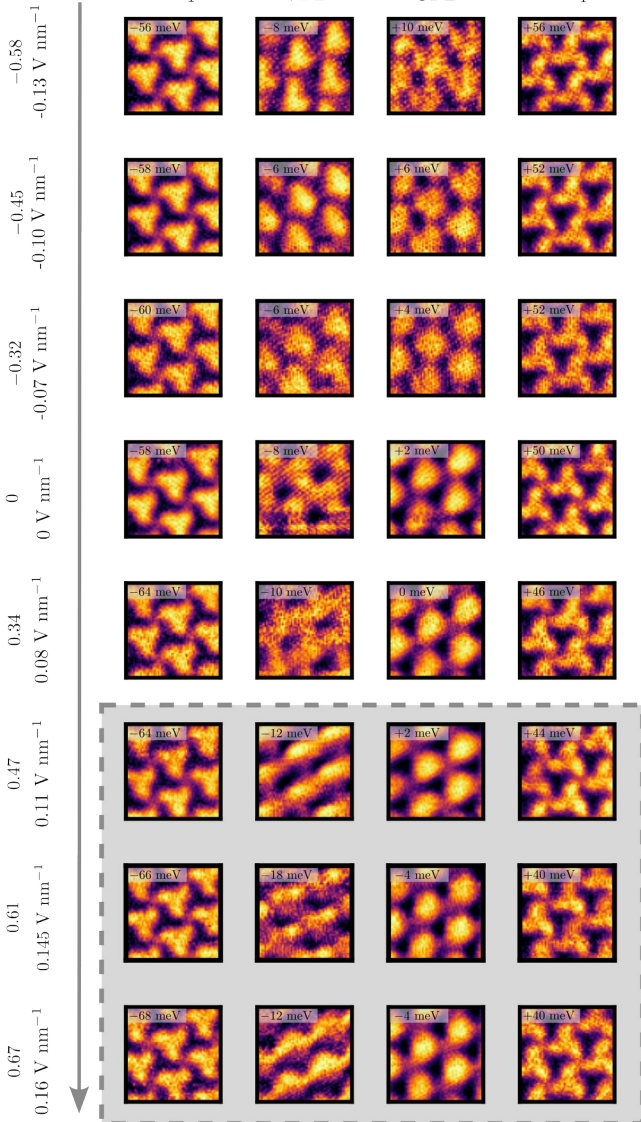
Preprocessing of D_{exp}



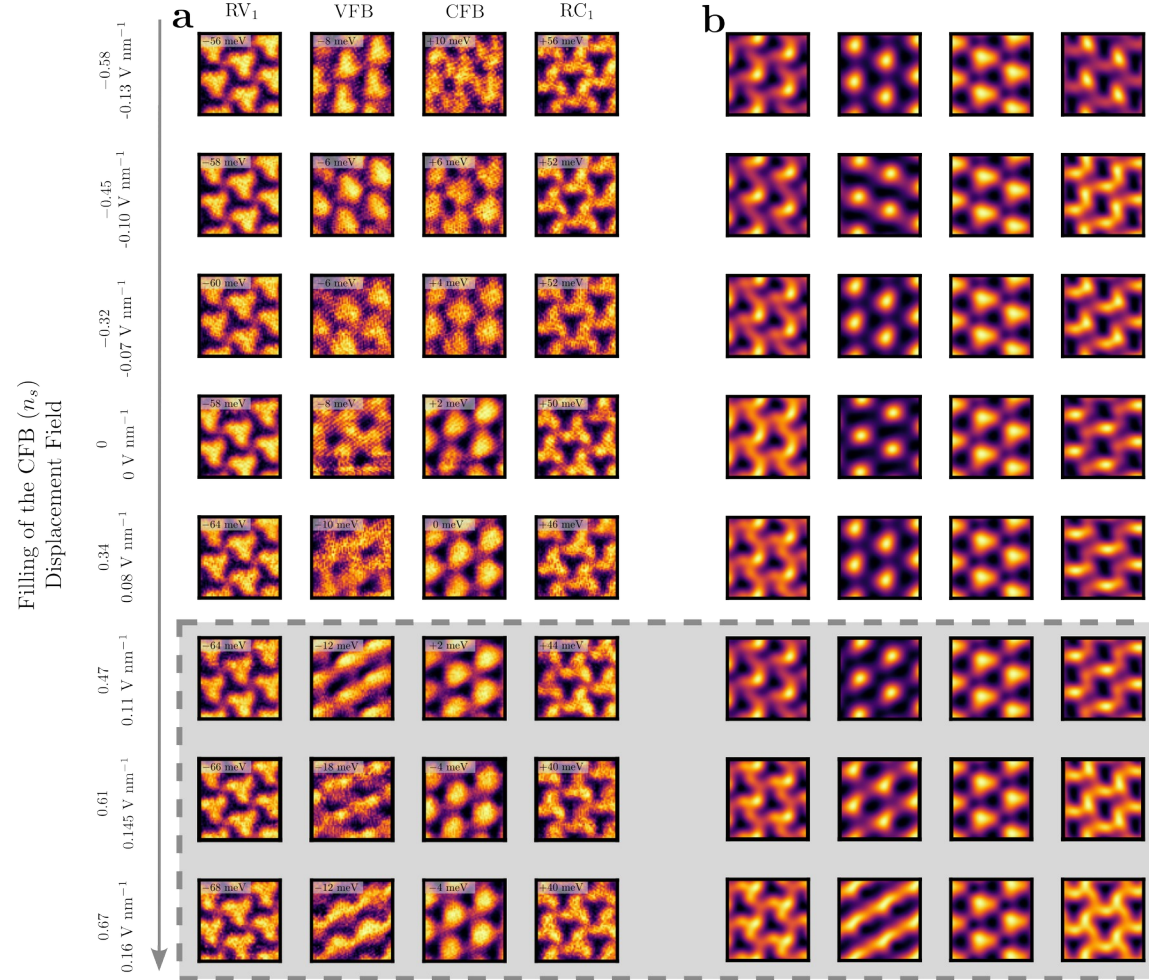
Predictions on D_{exp}



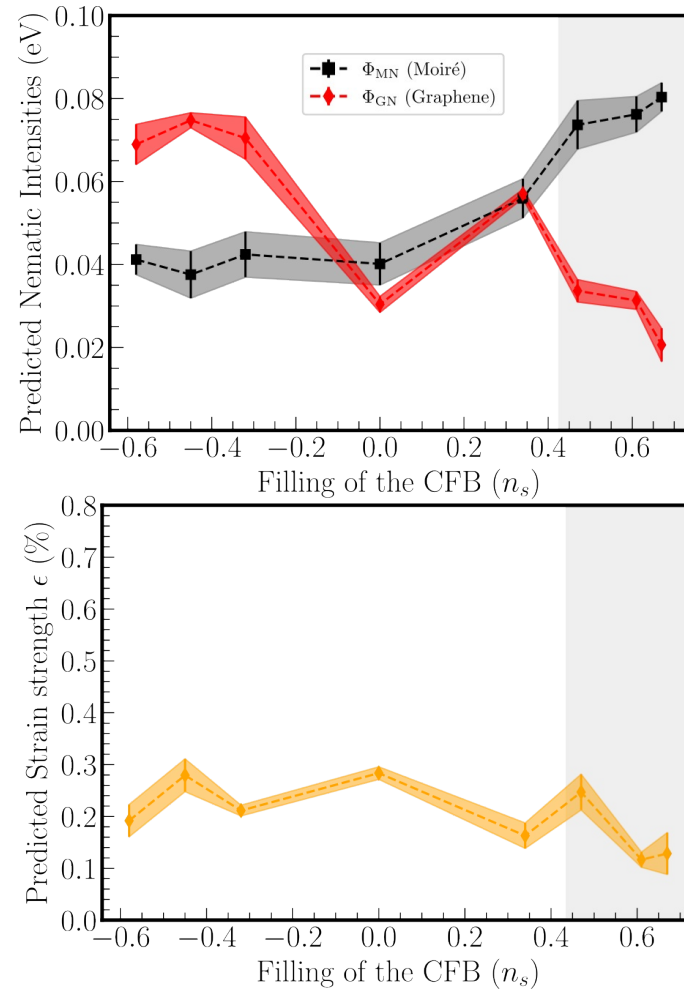
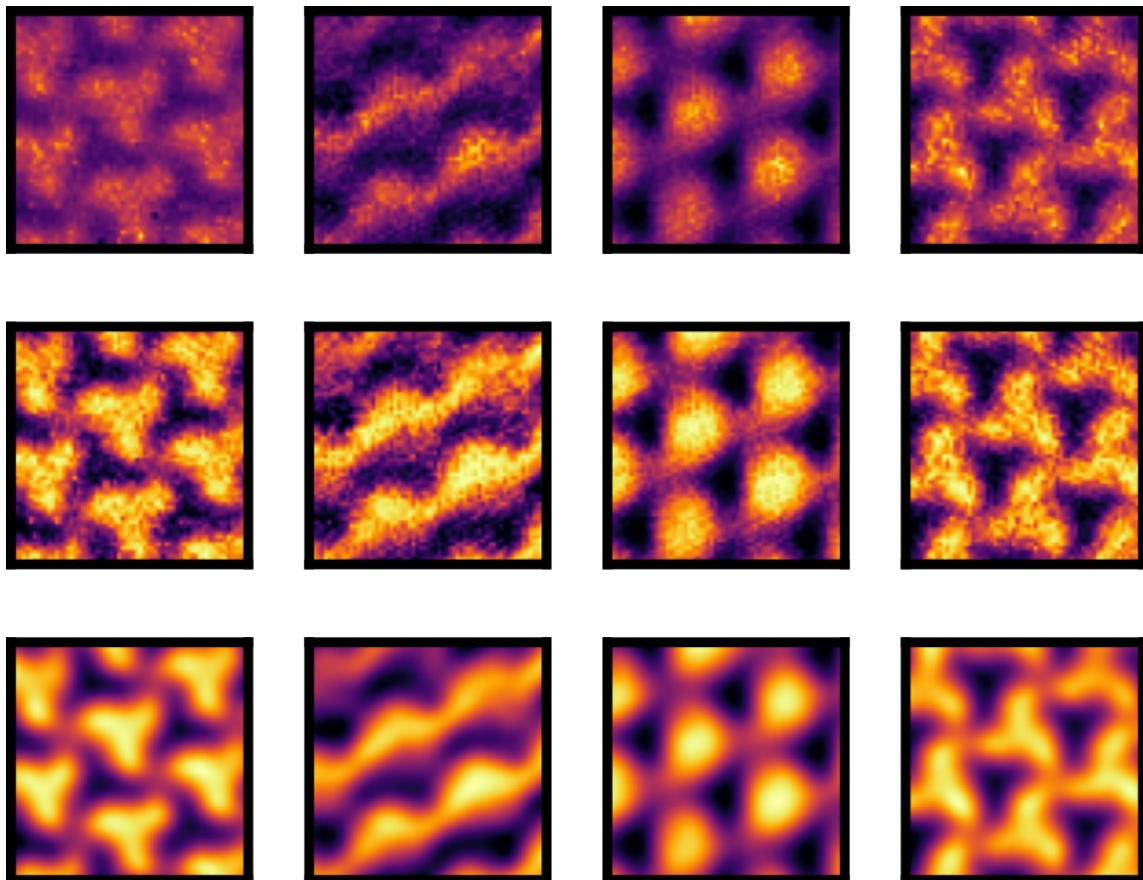
Filling of the CFB (n_s)
Displacement Field



Predictions on D_{exp}



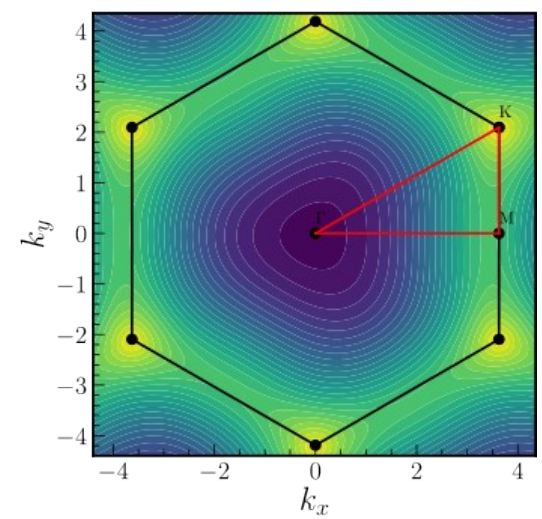
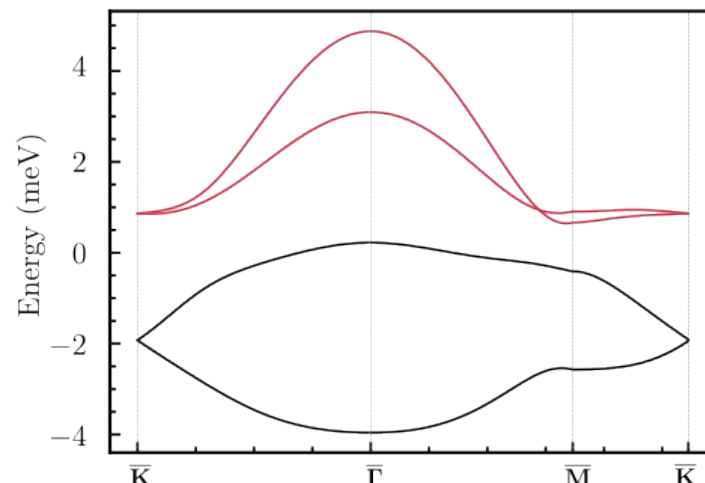
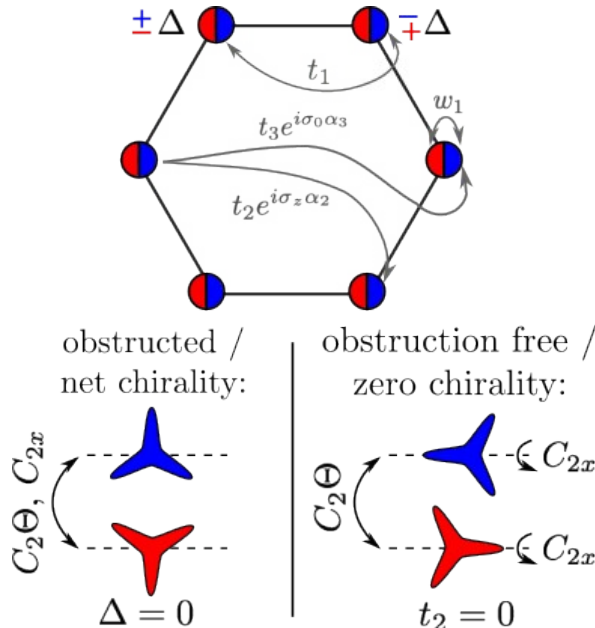
Prediction on D_{exp} (Preprocessing stage)



Beyond TDBG and the continuum model

Minimal tight-binding model (four bands per spin & valley)

$$H = \sum_{\vec{k}} \sum_{l=1,2} c_{\vec{k},l}^\dagger \vec{g}_{\vec{k}}^l \cdot \vec{\rho} c_{\vec{k},l}^\dagger + w_1 \sum_{\vec{k}} \left(e^{-i\theta_w} c_{\vec{k},1}^\dagger c_{\vec{k},2} + \text{H.c.} \right),$$



Beyond TDBG and the continuum model

Nematic order

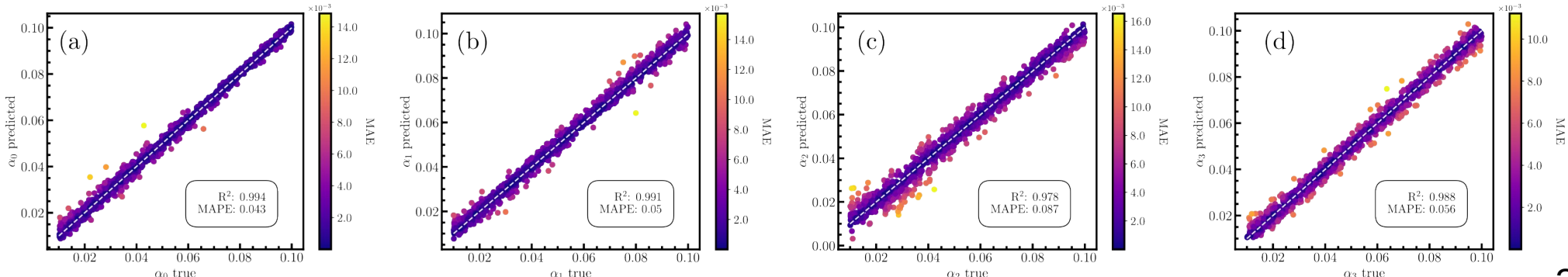
$$\Delta h_{\mathbf{k}} = \phi \cdot \mathbf{g}_{\mathbf{k}} = \phi_1 g_{1,\mathbf{k}} + \phi_2 g_{2,\mathbf{k}}$$

$$\begin{aligned} \mathbf{g}_{\mathbf{k}} \equiv \begin{pmatrix} g_{1,\mathbf{k}} \\ g_{2,\mathbf{k}} \end{pmatrix} &= \alpha_0 \rho_0 \sigma_0 \begin{pmatrix} f_{1,\mathbf{k}} \\ f_{2,\mathbf{k}} \end{pmatrix} + \alpha_1 \rho_0 \sigma_x \begin{pmatrix} f_{1,\mathbf{k}} \\ f_{2,\mathbf{k}} \end{pmatrix} \\ &+ \alpha_2 \rho_0 \sigma_y \begin{pmatrix} -f_{2,\mathbf{k}} \\ f_{1,\mathbf{k}} \end{pmatrix} + \alpha_3 \rho_z \sigma_z \begin{pmatrix} -f_{2,\mathbf{k}} \\ f_{1,\mathbf{k}} \end{pmatrix} \end{aligned}$$

Learn $\alpha_0, \alpha_1, \alpha_2, \alpha_3$

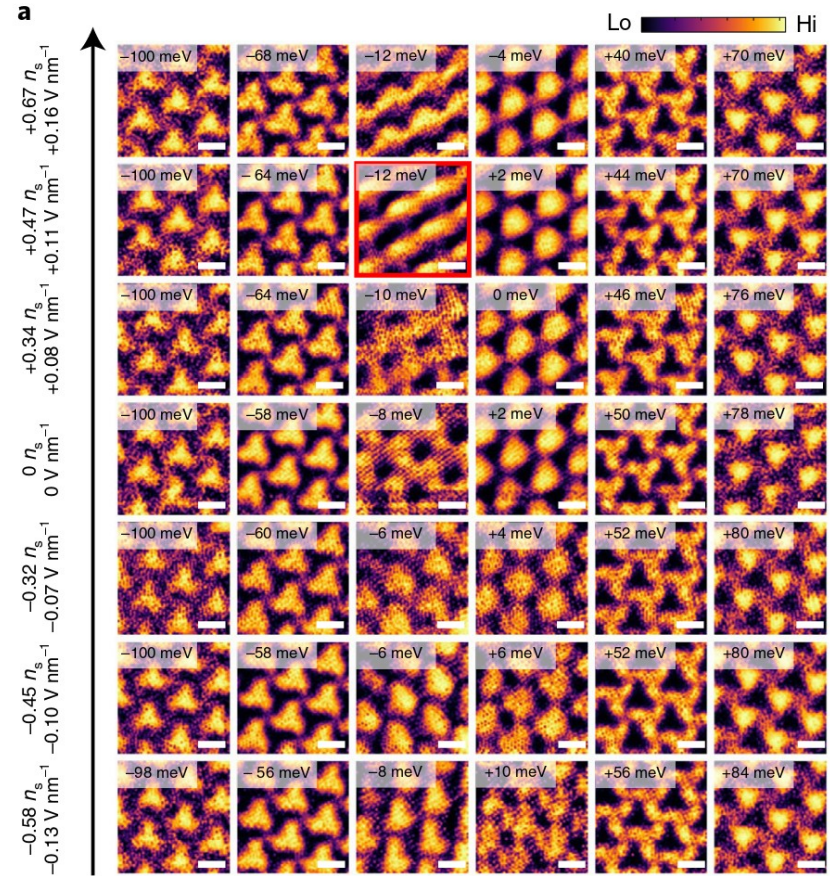
if we focus on leading lattice harmonic

$$\mathbf{f}_{\mathbf{k}} = \frac{8}{3} \left(\cos k_y - \cos \frac{\sqrt{3}k_x}{2} \cos \frac{k_y}{2}, \sqrt{3} \sin \frac{\sqrt{3}k_x}{2} \sin \frac{k_y}{2} \right)^T$$



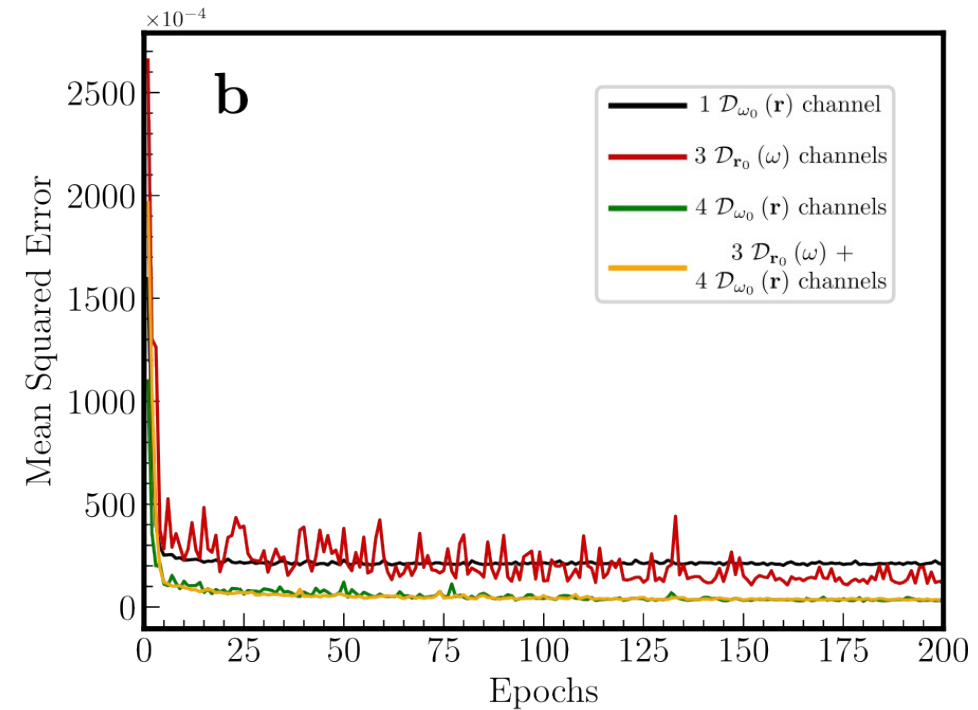
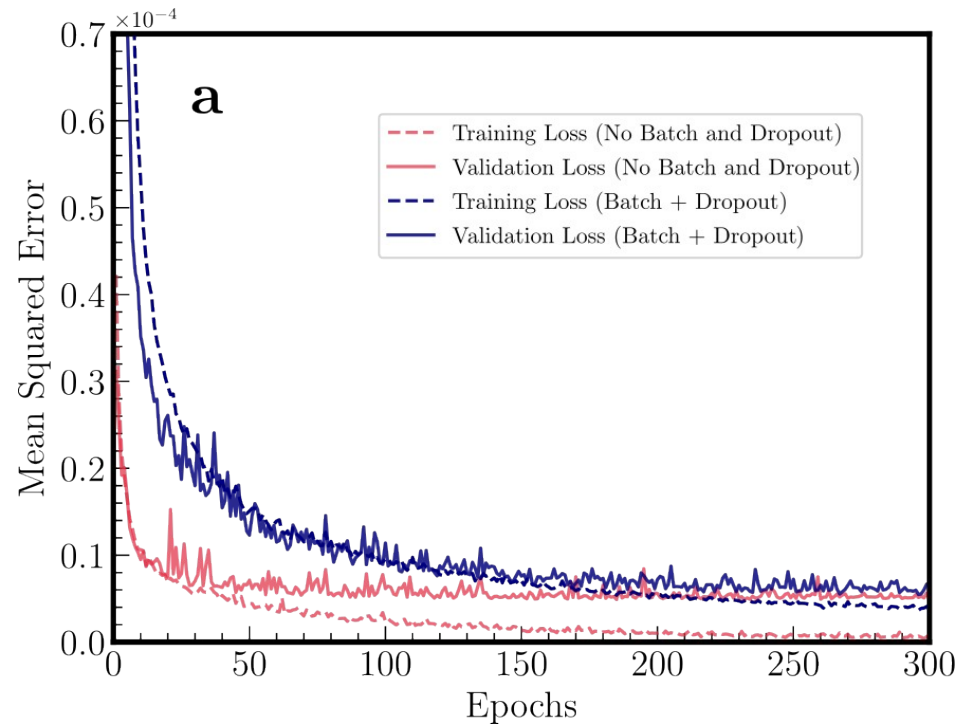
Overview and Outlook

- CNN's can distinguish nematicity and strain influence. How to
- Possible crossover between GN and MN for TDBG;
- Applicability beyond the continuum model and TDBG;
- Microscopic parameter learning from data (kind of Hamiltonian Learning);
 - Automated analysis of larger datasets;
 - Extensible to a variety of experimental setups? Comparison between different theoretical models?

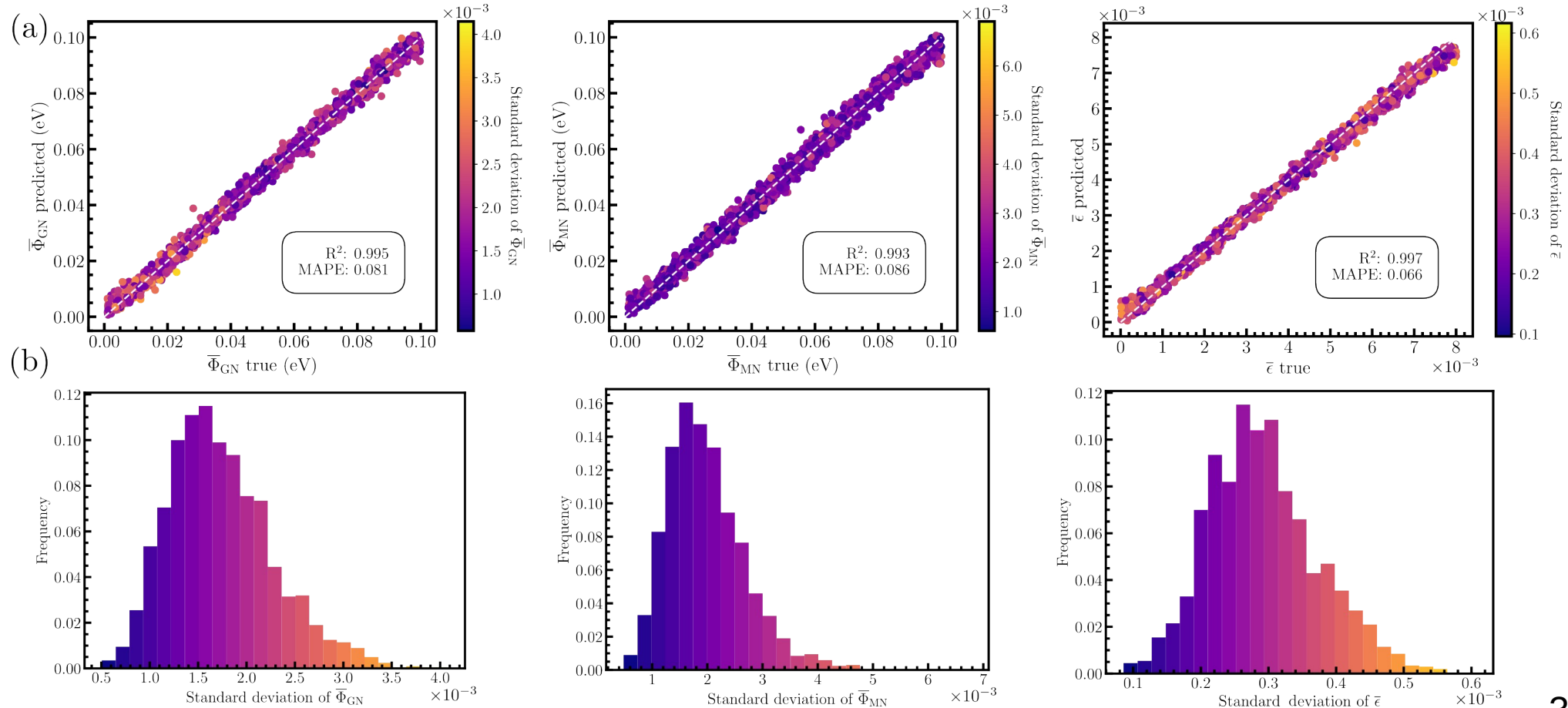


Backup slides

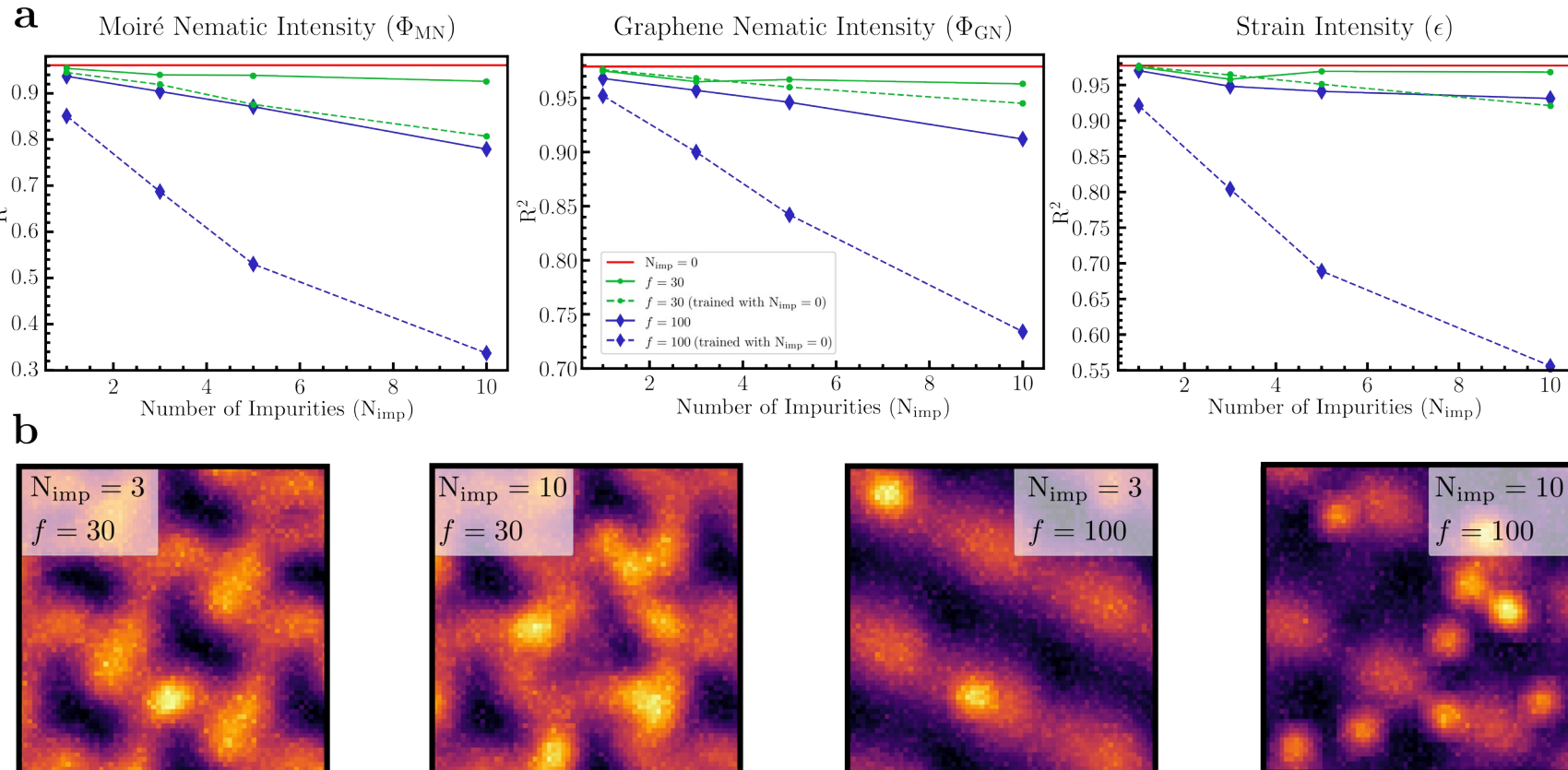
Number of channels and overfitting



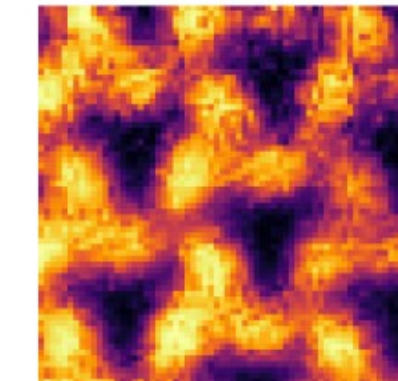
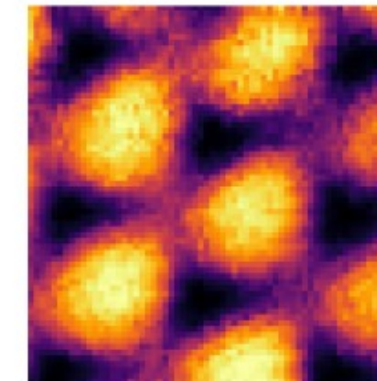
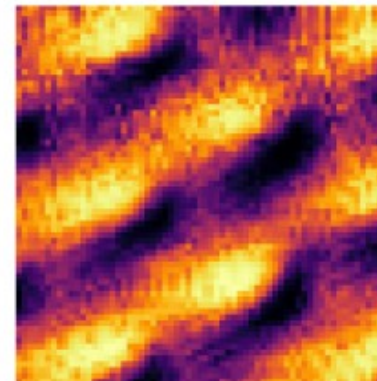
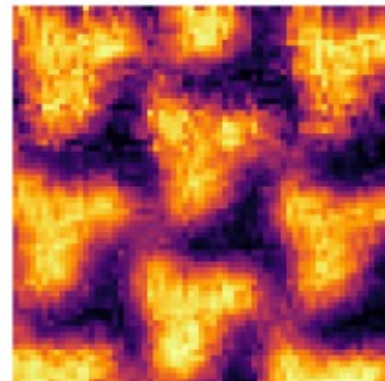
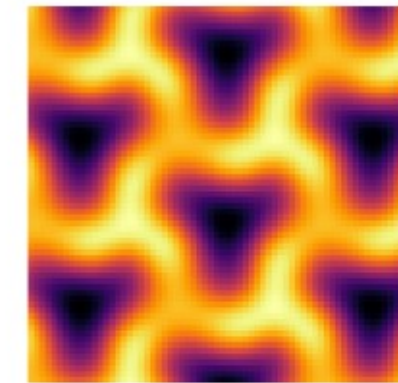
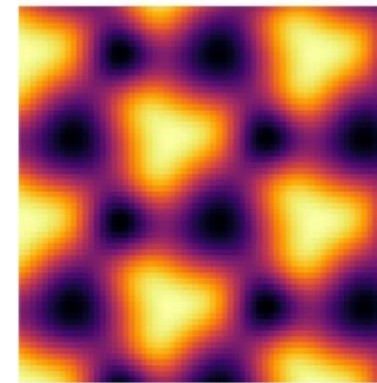
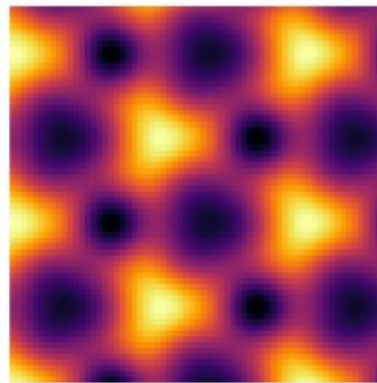
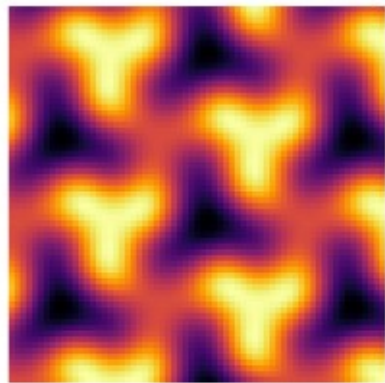
Average over different runs



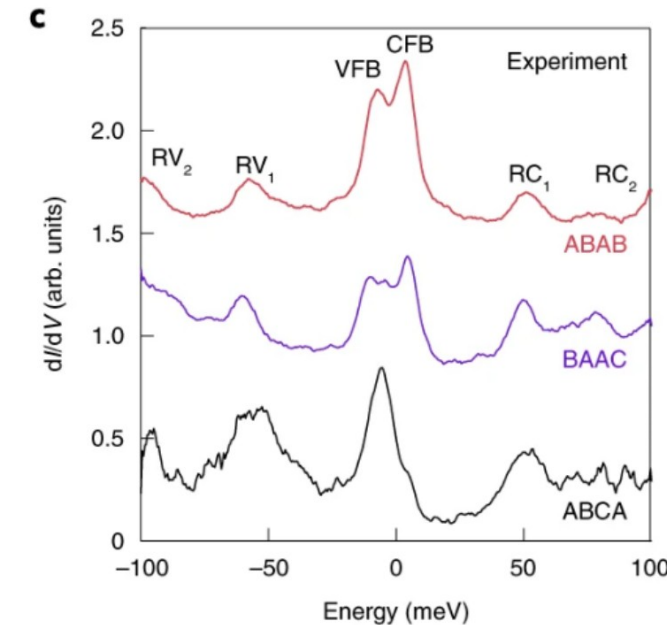
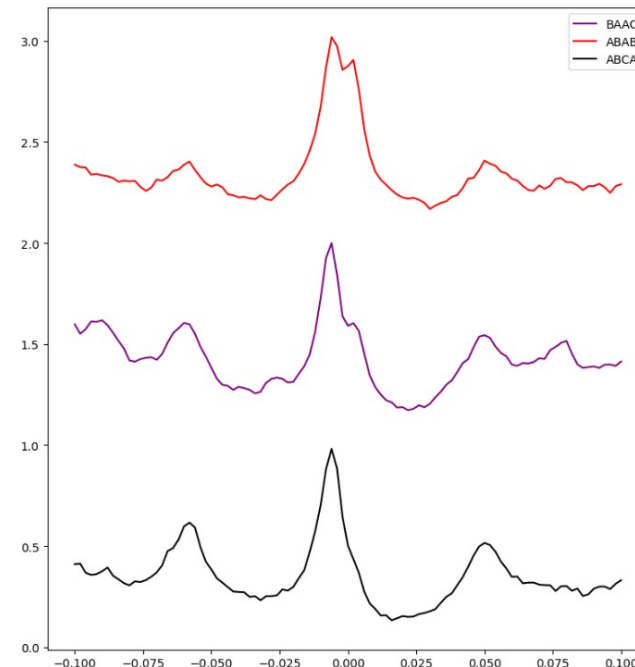
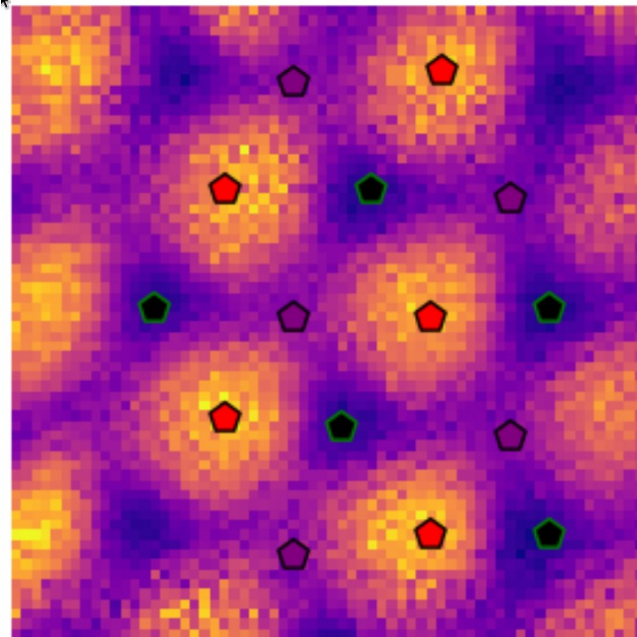
Robustness regarding impurities



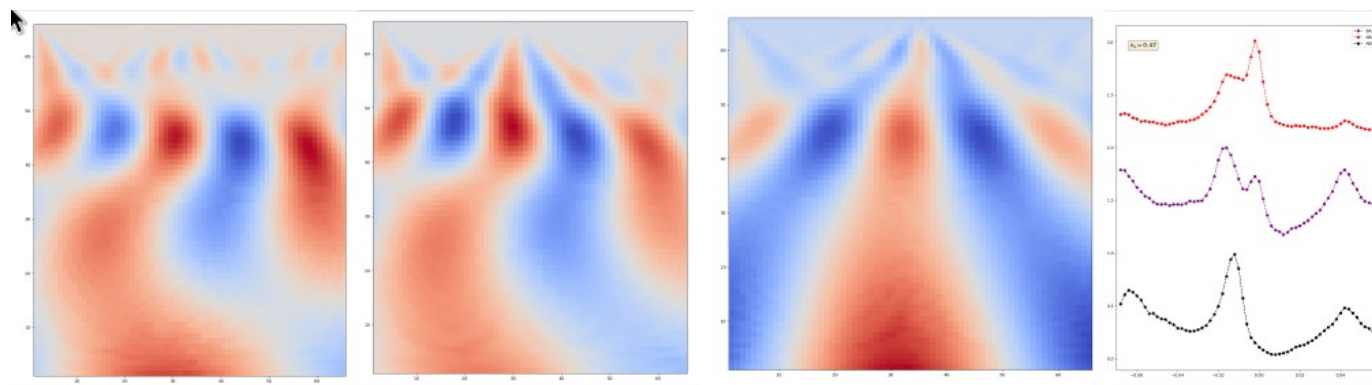
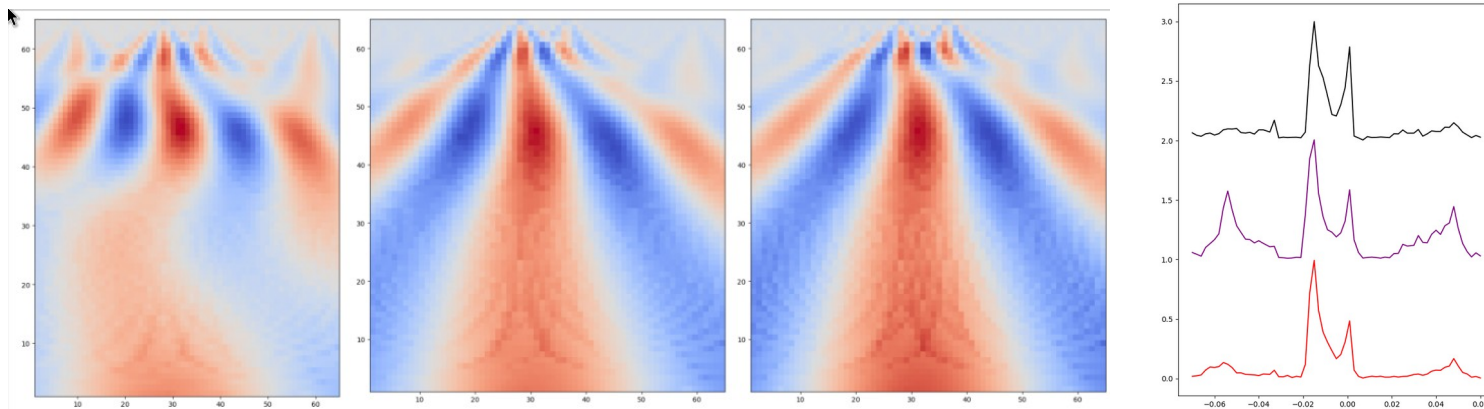
Preprocessing of the experimental data



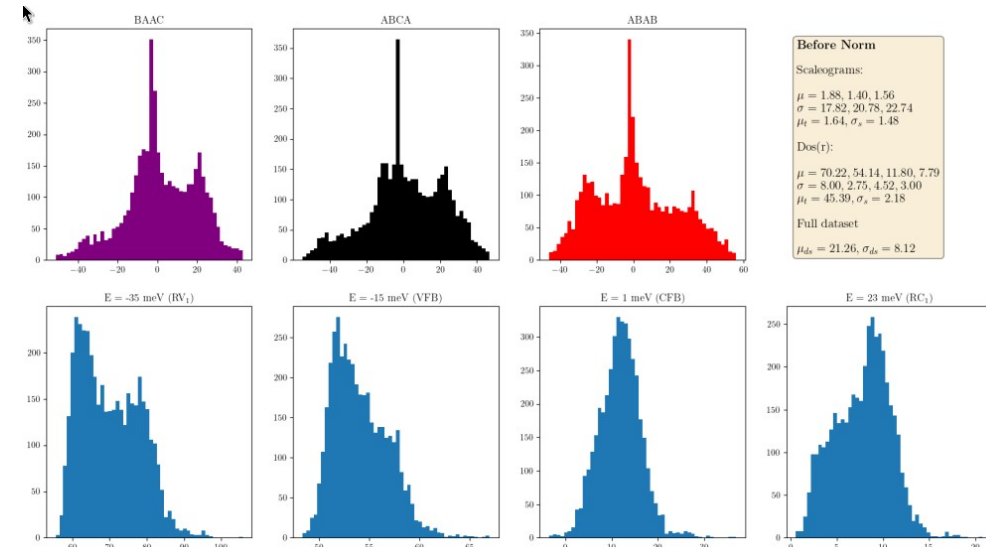
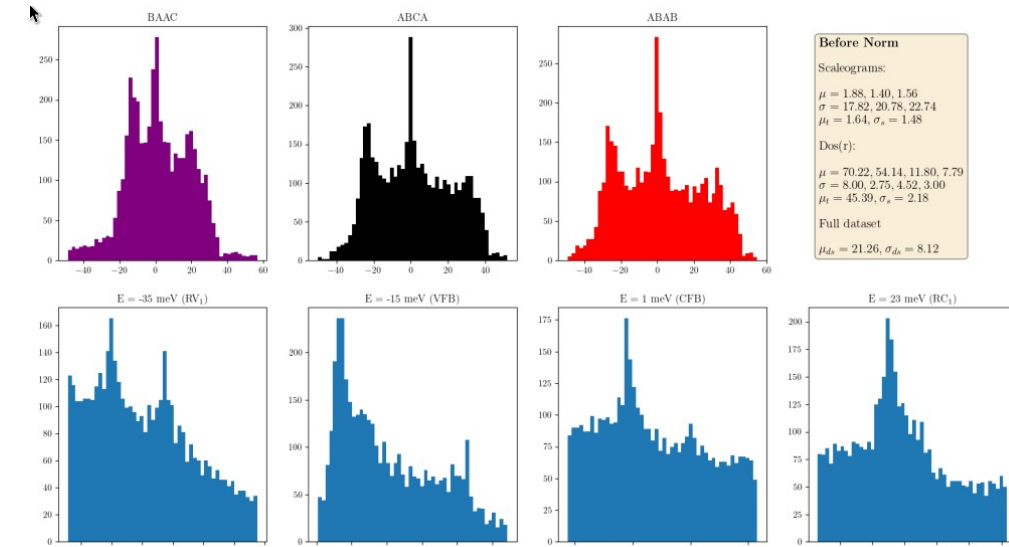
Preprocessing of the experimental data



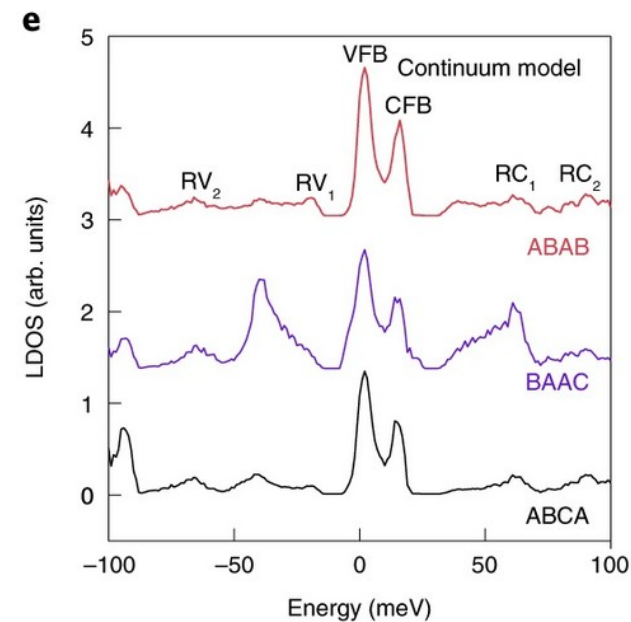
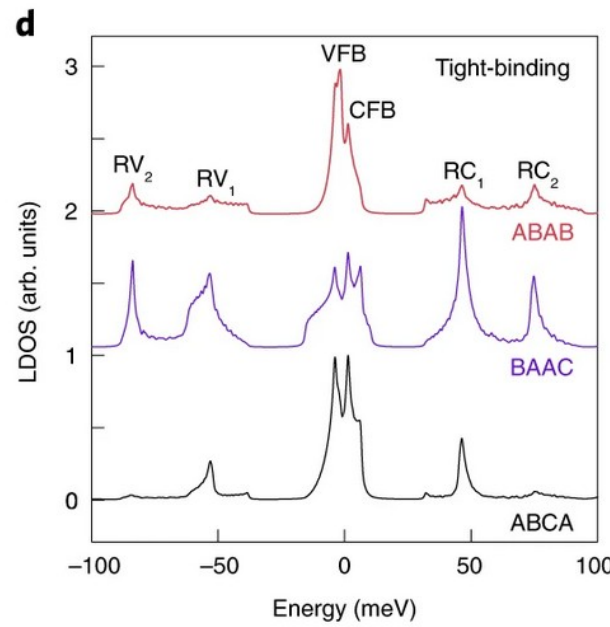
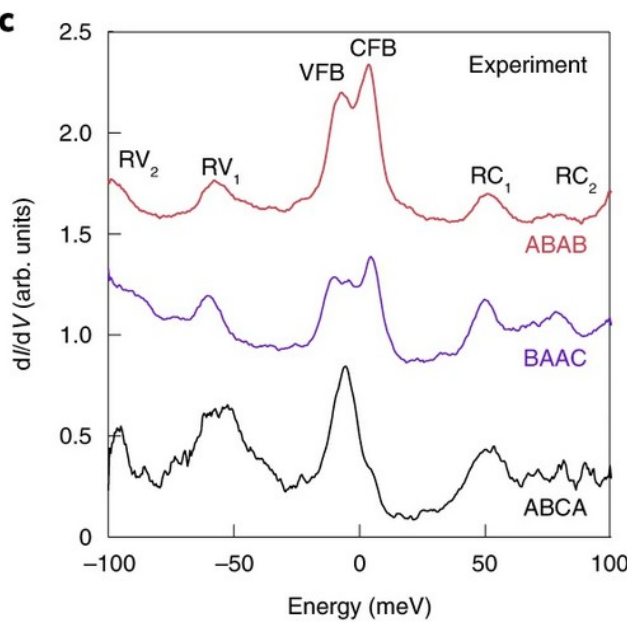
Preprocessing of the experimental data



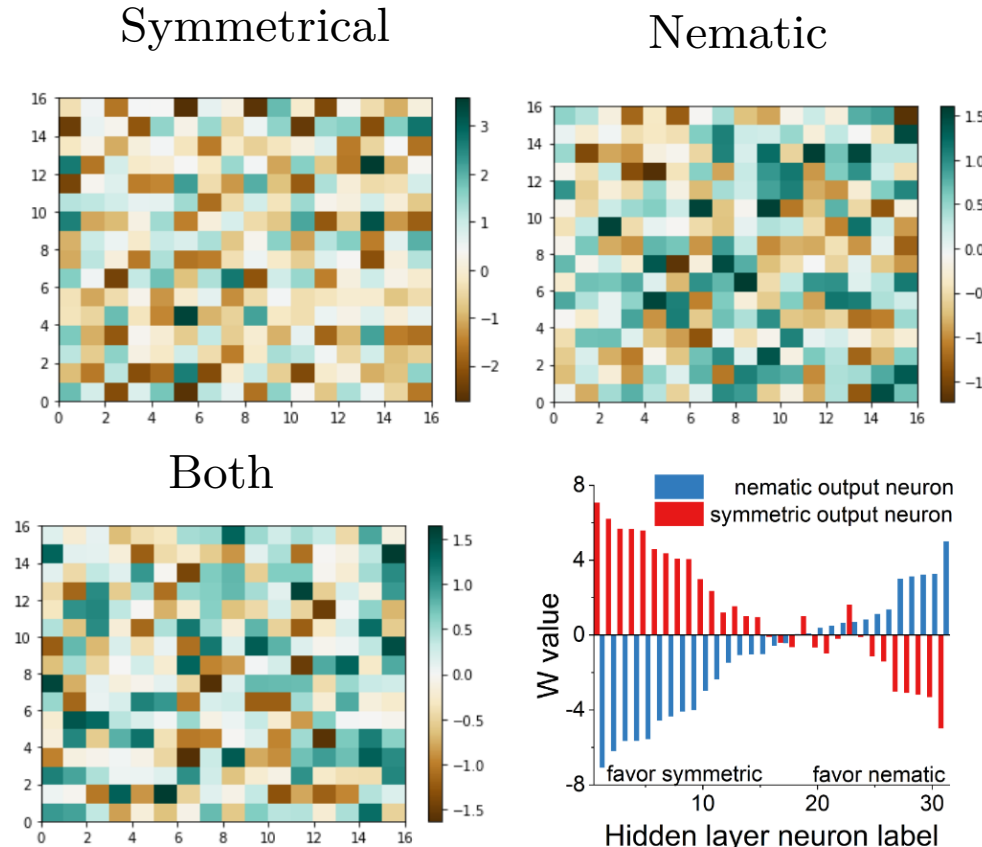
Preprocessing of the experimental data



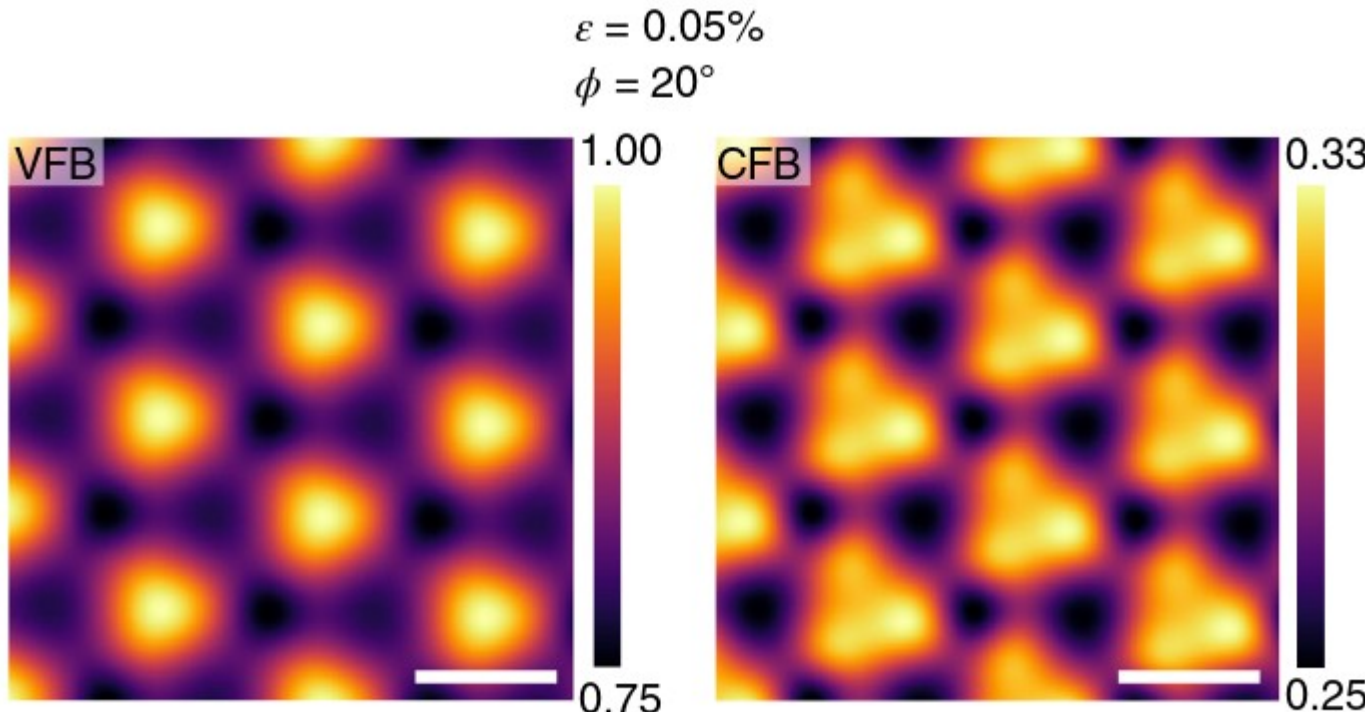
Limitations of theoretical model/data resolution



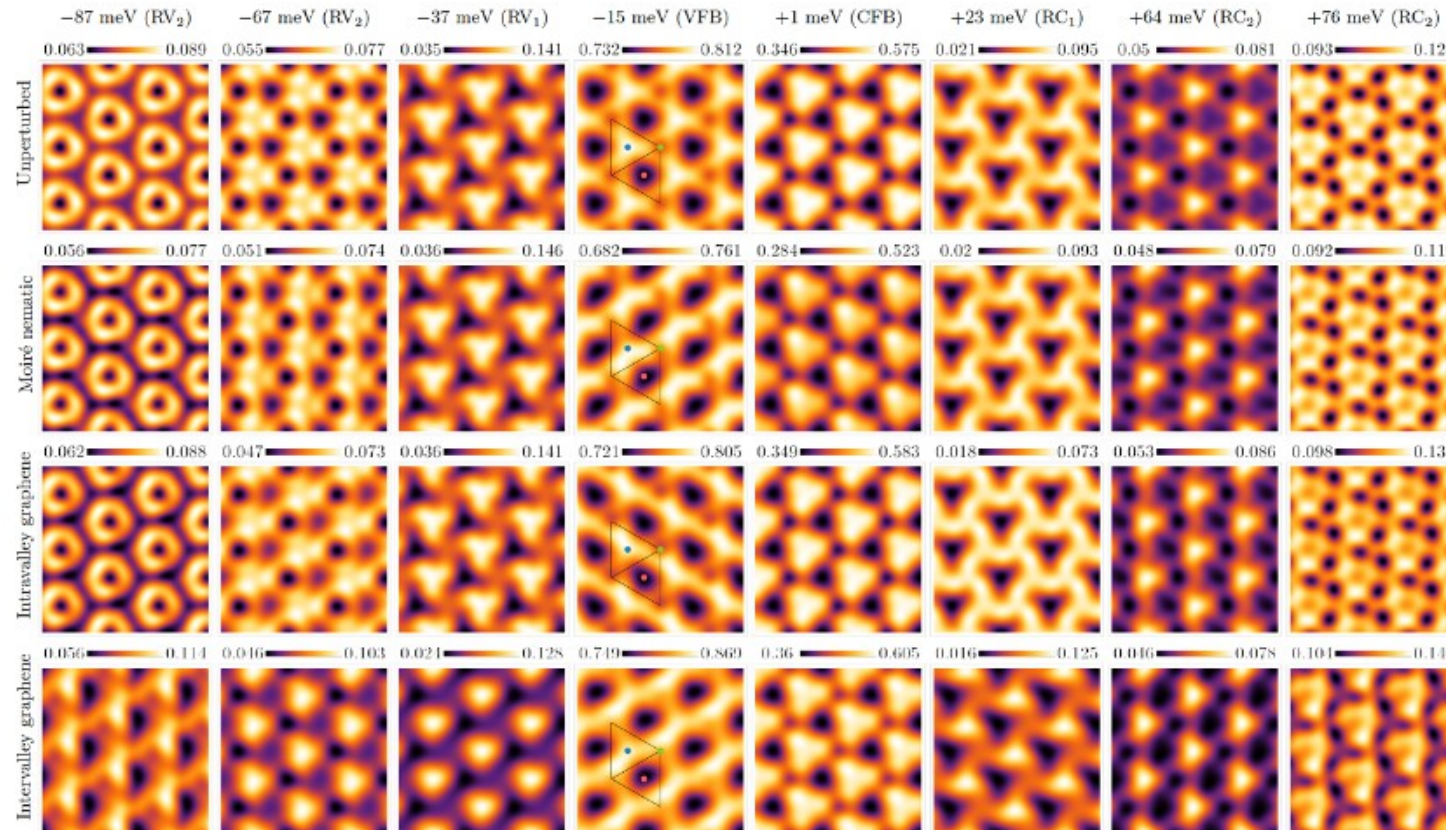
Interpretability? Correlations in AI nematic study



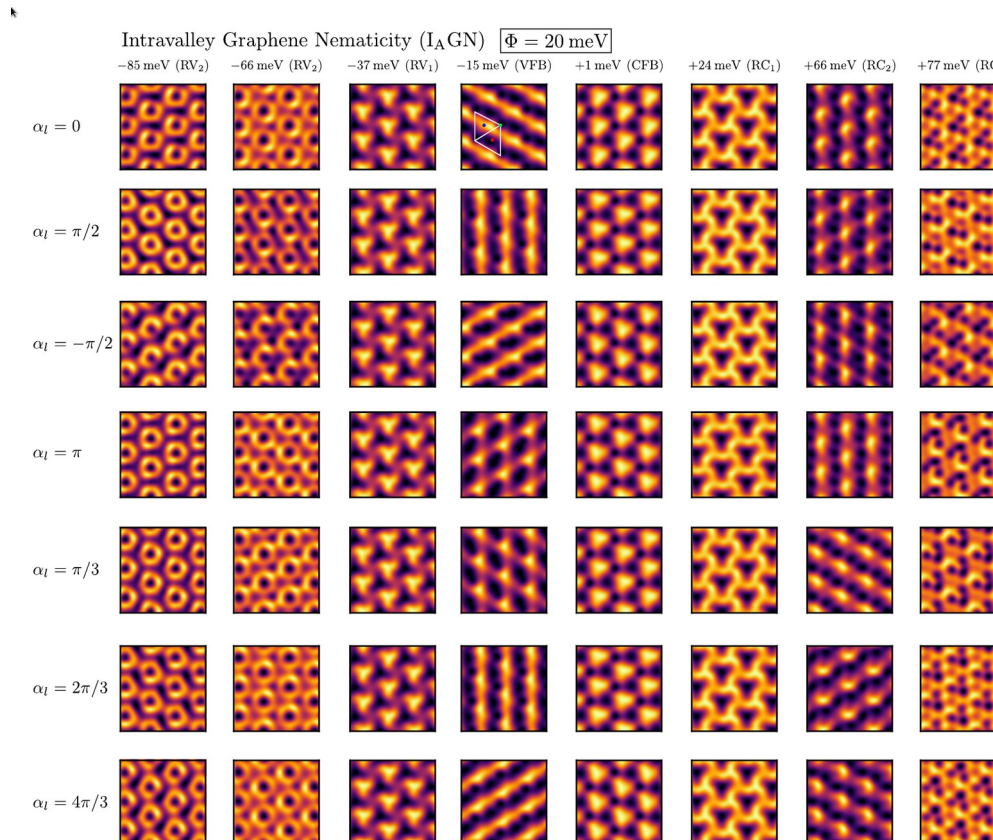
Tight Binding in TDBG



More nematic couplings: Intervalley GN



More nematic couplings: Intervalley GN



R. Samajdar, M. S. Scheurer, S. Turkel, et al. 2D Materials 8, 034005 (2021).